RMetS
Royal Meteorological Society

Review Article
Entrainment and detrainment in cumulus convection: an overview

Wim C. de Rooy,[a]* Peter Bechtold,[b] Kristina Fröhlich,[c] Cathy Hohenegger,[d] Harm Jonker,[e] Dmitrii Mironov,[c] A. Pier Siebesma,[a,e] Joao Teixeira[f] and Jun-Ichi Yano[g]

[a]*Royal Netherlands Meteorological Institute (KNMI), De Bilt, The Netherlands*
[b]*European Centre for Medium Range Weather Forecasts, Reading, UK*
[c]*Deutscher Wetterdienst, Offenbach am Main, Germany*
[d]*Max Planck Institute for Meteorology, Hamburg, Germany*
[e]*Department of Multi-Scale Physics, Delft University of Technology, The Netherlands*
[f]*Jet Propulsion Laboratory, California Institute of Technology, Pasadena, California*
[g]*GAME/CNRM, CNRS-INSU-MétéoFrance, URA 1357, Toulouse, France*

*Correspondence to: W. C. de Rooy, KNMI, PO Box 201, 3730 AE De Bilt, The Netherlands. E-mail: rooyde@knmi.nl

Entrainment and detrainment processes have been recognised for a long time as key processes for cumulus convection and have recently witnessed a regrowth of interest mainly due to the capability of large-eddy simulations (LES) to diagnose these processes in more detail. This article has a twofold purpose. Firstly, it provides a historical overview of the past research on these mixing processes, and secondly, it highlights more recent important developments. These include both fundamental process studies using LES aiming to improve our understanding of the mixing process, but also more practical studies targeted toward an improved parametrised representation of entrainment and detrainment in large-scale models. A highlight of the fundamental studies resolves a long-lasting controversy by showing that lateral entrainment is the dominant mixing mechanism in comparison with the cloud-top entrainment in shallow cumulus convection. The more practical studies provide a wide variety of new parametrisations with sometimes conflicting approaches to the way in which the effect of the free tropospheric humidity on the lateral mixing is taken into account. An important new insight that will be highlighted is that, despite the focus in the literature on entrainment, it appears that it is rather the detrainment process that determines the vertical structure of the convection in general and the mass flux especially. Finally, in order to speed up progress and stimulate convergence in future parametrisations, stronger and more systematic use of LES is advocated.

Key Words: large-eddy simulation; parametrisations; lateral mixing

Received 3 January 2012; Revised 26 March 2012; Accepted 28 March 2012; Published online in Wiley Online Library 7 June 2012

Citation: de Rooy WC, Bechtold P, Fröhlich K, Hohenegger C, Jonker H, Mironov D, Siebesma AP, Teixeira J, Yano J-I. 2013. Entrainment and detrainment in cumulus convection: an overview. *Q. J. R. Meteorol. Soc.* **139**: 1–19. DOI:10.1002/qj.1959

1. Introduction

It is difficult to overemphasise the importance of cumulus convection in climate and weather. It is a key process in the hydrological and energy cycle through the vertical transport of heat, moisture and momentum, it determines precipitation and the clouds associated with the moist convection directly, and largely affects the global energy

balance through interaction with the solar radiation. As most state-of-the-art numerical weather prediction (NWP) and climate models have insufficient resolution to resolve cumulus cloud-related processes, these need to be incorporated in a statistical way through the use of parameterisations in terms of the resolved variables.

The most common way to parametrise the vertical transport of heat, moisture and momentum is through the use of so-called mass flux schemes. In short, in such schemes the updraught strength of a cumulus ensemble is characterised by a mass flux that quantifies the amount of mass that is transported in the vertical. Combining this mass flux with a cloud updraught model for temperature, moisture and momentum allows for the determination of the parametrised convective transport of these quantities. A key process that modifies the mass flux and the variables of the cloud updraught model is the mixing between clouds and their environment by the so-called entrainment and detrainment processes that describe respectively the inflow of environmental air into the cloud and the outflow of cloudy air into the environment. The precise nature of these mixing processes is still an active field of research and their parametrisation is still in its infancy. Sensitivity studies with climate models (Murphy *et al.*, 2004; Klocke *et al.*, 2011) in which the values of many parametrised processes are varied, have demonstrated that the mixing processes in cumulus convection are amongst the most sensitive.

In accordance with their importance, numerous articles on entrainment and detrainment have appeared over the last 65 years. In this article the developments are described which we believe are important, with a focus on the more recent studies. However, in view of the large extent of the field, we do not claim to give a complete overview of all notable studies.

Nowadays the mass flux concept is also used for dry convection in the increasingly popular eddy diffusivity mass flux (EDMF) schemes (Soares *et al.*, 2004; Siebesma *et al.*, 2007). Nevertheless, lateral mixing in dry convection will not be considered here.

We will start with a historical overview of studies concerning lateral mixing in cumulus convection in section 2. The subsequent sections describe some recent developments which can roughly be divided into studies aiming at a better fundamental understanding of how the mixing processes take place (section 3) and studies that are more targeted towards a better representation of lateral mixing within a parametrization context. (section 4). We believe both type of studies are important and relevant. Section 3 starts by making precise notions of the lateral mixing processes. The rest of this section concerns several large-eddy simulation (LES) studies to explore these mixing processes in a fundamental way. Section 4 describes a selection of studies relevant for the parametrization of lateral mixing in NWP and climate models. The focus in this section shifts from shallow (i.e. virtually non-precipitating) convection in sections 4.1 and 4.2, to the differences between shallow and deep (i.e. precipitating) convection in section 4.3, to general research relevant for shallow and deep convection (sections 4.4, 4.5). Finally, in section 5 the conclusions and discussions are presented.

2. History

The importance of lateral mixing in cumulus convection has been recognised for a long time, starting with the seminal paper of Stommel (1947). However, it turned out to be a challenging subject since some of the fundamental questions related to it are still a matter of debate. This applies, for instance, to the question of whether cumulus convection should be represented by a bubble or a plume, a topic already discussed by Squires and Turner (1962), and also to whether the dilution of the cloudy updraught is predominantly caused by lateral or cloud-top entrainment. Furthermore, whereas early studies concentrated more on the mixing of a single cloud, nowadays due to its application in parametrisations in NWP and climate models there is a need to describe the effect of lateral mixing for a whole cumulus ensemble.

2.1. *Thermal or plume?*

As mentioned above, Squires and Turner (1962) discussed the differences between the plume or jet and the bubble as a thermal concept for describing convection. Looking at a large thunderstorm with its rather tall and slender current, they suggested an analogy with a steady-state buoyant turbulent plume, having a continuous source of heat from below cloud base and no significant mixing at cloud top. On the other hand, for small clouds, being about as deep as wide, a non-steady bubble model seemed more appropriate in which the air in the wake near the top will be the dominant mixing process. In line with the current general view, Squires and Turner (1962) presumed that a realistic model of cumulus convection should include features of both models. Nevertheless, contemporary convection schemes mainly possess the characteristics of a plume model.

2.2. *Distinguishing different lateral mixing processes*

Dilution of a cumulus cloud by entrainment of environmental air was described for the first time by Stommel (1947). After Stommel, numerous observational studies of cumulus clouds with aircraft followed (e.g. Warner, 1955). In these studies, entrainment strength was quantified through the ratio between the measured liquid water and its adiabatic value, and they provided observational evidence of the entrainment of drier air from outside the cloud.

More precise quantitative descriptions of entrainment originated from laboratory water tank experiments of thermal plumes (Morton *et al.*, 1956; Turner, 1963) describing an increasing mass flux M with height,

$$\frac{1}{M}\frac{\partial M}{\partial z} = \varepsilon \simeq \frac{0.2}{R}, \tag{1}$$

where ε denotes the fractional entrainment, R is the radius of the rising plume and $M = \rho w_c a_c$ (kg m^{-2}s^{-1}) denotes the upward mass flux consisting of the product of the density ρ, the plume updraught velocity w_c and the associated plume fractional area a_c. We deliberately choose here the suffix c as, in the remainder of this article, we will associate the updraught properties with cloudy updraughts. According to (1), larger thermals (clouds) have smaller fractional entrainment, which is a consequence of the fact that larger areas have a relatively smaller perimeter. Many of

the early (but also more recently developed) cloud models use entrainment rates still based on this entraining plume model.

An important further refinement on the entrainment formulation (1) was first pointed out by Houghton and Cramer (1951). They made a distinction between dynamical entrainment due to larger-scale organised inflow (noted as ε_{dyn}) and turbulent entrainment caused by turbulent mixing at the cloud edge (noted as $\varepsilon_{\text{turb}}$):

$$\frac{1}{M}\frac{\partial M}{\partial z} = \varepsilon_{\text{dyn}} + \varepsilon_{\text{turb}}. \tag{2}$$

Whereas the first type of entrainment has the characteristics of advective transport across the interface, turbulent entrainment is of diffusive nature and is therefore often described with an eddy diffusivity approach (Kuo, 1962; Asai and Kasahara, 1967). Since the dynamical and turbulent fractional entrainment rates are by definition positive, they cause the mass flux to increase with height. This is in agreement with old water tank experiments without stratification where all laterally entrained fluid was considered to be part of the bubble. Here the bubble was defined as a turbulent fluid in contrast with the non-turbulent environment of the bubble. For rising dry thermals, a similar argument might hold. However cumulus clouds contain liquid water and evaporative cooling plays an important role in the mixing process. Due to the mentioned turbulent mixing at the cloud edge, a mixture of in-cloud and environmental air is developed. This mixture can become negatively buoyant by evaporative cooling and will in this case detrain from the cloud (possibly after some time), represented by δ_{turb}. In tank experiments with stratification, as well as for clouds in the atmosphere, the cloud or thermal itself can also become negatively buoyant. As a result, it stops rising and is usually dissolved in the environment. This process is called massive or dynamical detrainment and is represented by δ_{dyn}. So, if we finally include all distinguished mixing processes, the change of the mass flux with height can be written as

$$\frac{1}{M}\frac{\partial M}{\partial z} = \varepsilon_{\text{dyn}} + \varepsilon_{\text{turb}} - \delta_{\text{dyn}} - \delta_{\text{turb}}. \tag{3}$$

2.3. *Steady-plume assumption*

As mentioned above, most contemporary convection schemes have adopted the entraining/detraining plume concept. In the traditional plume model, several assumptions are made. First of all, the interior of individual plumes is considered to be homogeneous, so just entrained air is homogeneously mixed instantaneously. Observations (e.g. Ludlam and Scorer, 1953) as well as LES (Zhao and Austin, 2005a; Heus *et al.*, 2009a) show that especially large clouds (with longer life times) are a succession of bubbles rising from roughly the same place, each penetrating further than its predecessor. This will result in an inhomogeneous interior of individual plumes. Secondly, the entraining/detraining plume model assumes a steady state. However, in reality, clouds experience a life cycle with time-scales mainly related to cloud size. For example, a decaying cloud at the end of its life will have completely different characteristics from a still developing cloud. The steady state assumption is more valid if, instead of single clouds, we consider the overall impact of a (large) cloud ensemble containing all cloud sizes and clouds in different stages of their life cycle. Moreover, considering the contemporary grid sizes of climate and most NWP models, convection schemes should actually describe the overall effect of an ensemble of clouds rather than a single cloud. Historically, a steady state plume model has been considered a reasonable starting point for describing a cloud ensemble.

A first example how this can be done, and still the basis for several existing convection schemes (e.g. Wagner and Graf, 2010), is the seminal work of Arakawa and Schubert (1974). They assumed that the change of the large-scale (in the model context, grid-point) properties is slow in comparison with the response of individual clouds, called quasi-equilibrium. Further, Arakawa and Schubert (1974) described the overall transport by an ensemble of entraining plume-like cumuli rising to different heights because they have a spectrum of initial sizes and hence different entrainment rates, defined by (1). However, most contemporary mass flux parametrisations employ a so-called bulk approach in which all active cloud elements are represented in one steady state updraught representing the whole cloud ensemble.

2.4. *Bulk plume convection parametrisations*

Numerous entrainment and detrainment parametrisations have been proposed for bulk mass flux schemes. Popular formulations proposed by Tiedke (1989), Gregory and Rowntree (1990), Nordeng (1994) and Bechtold *et al.* (2008) can be ordered in terms of the right-hand side (RHS) of (3). Tiedke (1989) and Nordeng (1994) assume that $\varepsilon_{\text{turb}}$ and δ_{turb} are equal and given by (1), while in Bechtold *et al.* (2008), $\varepsilon_{\text{turb}}$ depends on the saturation specific humidity. Gregory and Rowntree (1990) also proposed (1) for $\varepsilon_{\text{turb}}$ but utilised a systematically smaller δ_{turb}. Dynamical entrainment ε_{dyn} is based on moisture convergence in Tiedke (1989), on momentum convergence in Nordeng (1994), on relative humidity in Bechtold *et al.* (2008) and absent in Gregory and Rowntree (1990). Organised detrainment is in general formulated as a massive lateral outflow of mass around the neutral buoyancy level, although the precise details differ in the various parametrisations. The above-cited parametrisations typically use (1) assuming a fixed radius of $R \simeq 500$ m for shallow clouds and $R \simeq 2000$ m for deep convection.

Another class of entrainment/detrainment parametrisations, which do not distinguish explicitly between dynamical and turbulent mixing, is based on the 'buoyancy sorting' concept introduced by Raymond and Blyth (1986). This concept was transformed into an operational parametrisation by Kain and Fritsch (1990) (section 4.1). In their parametrisation, an ensemble of mixtures of cloudy and environmental air is formed, where each ensemble member has a different concentration of environmental air. If resulting mixtures are positively buoyant, they remain in the updraught and are part of the entrainment process, while negatively buoyant mixtures are rejected from the updraught and are part of the detrainment process. A number of recently proposed shallow cumulus convection schemes are based on or make use of this buoyancy sorting concept (sections 4.1 and 4.2).

2.5. Lateral versus vertical mixing

Entrainment of environmental air into clouds tends to dilute cloud properties and degrade the buoyancy characteristics of cloudy air, both of which affect the vertical transport by clouds. Knowing the characteristics of the air entering the cloud, which is strongly related to knowing the source height of the entrained air, is therefore naturally regarded as a crucial issue. In this respect it is most surprising that two radically opposing views, referred here as 'lateral entrainment' versus 'cloud-top entrainment', have been able to coexist for a long time in the cloud science community. The origin of these views go back as least as far as Stommel (1947) (lateral entrainment) and Squires (1958) (cloud-top entrainment). In the former view, cloudy air, carrying the properties of the cloud base, gets continually diluted during its ascent by mixing air entrained into the cloud via the lateral cloud edges. It is this view that has served as the basis for parametrisations of moist convective transport in operational models. Conversely, in the cloud-top entrainment view, environmental air predominantly gets entrained at or near the top of the cloud, after which it descends in the cloud via penetrative downdraughts, finally diluting the rising cloudy air by turbulent mixing. A conceptual picture of how this could look is given in Figure 13.8 of Stull (1988). Clearly the two views sketched above differ enormously with respect to the source height of entrained air, and therefore they also crucially differ with respect to the properties of air that dilute the cloud. It should be noted that, in principle, the two views are not mutually exclusive since both mechanisms could be active at the same time, but the question really is which of the two mechanisms dominates. Also, a rather contrived argument would be needed to anticipate that the two mechanisms are equally effective.

Ample evidence for the importance of lateral entrainment can be found in the literature (e.g. Lin and Arakawa, 1997; Raga *et al.*, 1990). Also, though perhaps more indirectly, the lateral entrainment view derives justification from the appreciable predictive quality of the moist convective parametrisations that are based on it (e.g. Kain and Fritsch, 1993; Siebesma and Cuijpers, 1995). On the other hand, compelling observational evidence for the cloud-top entrainment view came from the elegant analysis of Paluch (1979), who plotted in-cloud values of conservative variables (total specific humidity and equivalent potential temperature) in a diagram which now carries her name. Rather than displaying significant scatter, the in-cloud values observed during a cloud transect at a particular level were found to collapse onto a distinct line. Such a 'mixing line' is commonly taken as strong evidence for a two-point mixing scenario: if one mixes air from two (but not more) different sources, any mixture must show up on a line in such a diagram due to the nature of conservative variables. By extrapolating the line, Paluch identified the two source levels as cloud-base and cloud-top (or a level significantly higher than the level of the cloud transect). It is important to note that, at face value, the analysis of Paluch seems to leave no room for significant lateral entrainment since mixing with more than two sources would yield significant scatter away from the mixing line. Later studies (e.g. Betts, 1982, 1985; Boatman and Auer, 1983; Lamontagne and Telford, 1983; Jensen *et al.*, 1985) confirmed the findings of Paluch, thus providing further support to the importance of cloud-top entrainment. The historical shift from a lateral entrainment view towards a cloud-top entrainment view can very clearly be noted in the overview article by Reuter (1986), for example.

Criticism and warning comments, not so much directed at the location of data points in the Paluch diagrams, but rather at the interpretation drawn from them, were given by Taylor and Baker (1991) and Siebesma (1998). Siebesma pointed to the strong self-correlation that exists in the conserved variables chosen for the Paluch diagrams, which makes it hard for the data *not to line up* (e.g. Figure 1 of Heus *et al.*, 2008). Taylor and Baker (1991) drew attention to the phenomenon of 'buoyancy sorting' which implies that essentially only a biased selection of data points can show up in Paluch diagrams. Simply put, a bias is introduced because it is less likely to observe buoyant air parcels coming from above, as well as it is unlikely to observe negatively buoyant parcels coming from below. Consequently most observed data points are related to buoyant parcels coming from below and negatively buoyant parcels from above. As explained in detail in their article, this effect puts serious limits to the possible values one can observe at a particular cloud level: essentially the data points are confined to a triangle that very much resembles a line. They conclude 'The graphical analysis of non-precipitating cloud composition shows that the apparent mixing line structure of single level in-cloud points on a conserved tracer diagram can result from a continuous series of entrainment events occurring throughout the cloud depth if buoyancy sorting is dominant throughout the flow'. In section 3.7, we discuss recent LES studies that seem to provide a final answer to the controversy between cloud-top and lateral mixing.

2.6. The use of LES to study entrainment and detrainment

Obtaining accurate observations of entrainment and detrainment is notoriously difficult. Nevertheless, inventive studies like Raga *et al.* (1990) and Yanai *et al.* (1973) linked observations to entrainment rates. However, the translation from observed lateral mixing coefficients to an appropriate ε and δ for use in a bulk mass flux framework is far from trivial. Fortunately, LES models have matured since the 1990s, initiating a strong revival of entrainment/detrainment studies. The resolution of these models is high enough to resolve the largest eddies, which are responsible for the majority of the convective transport. Comparison with various field observations such as those from the Barbados Oceanographic and Meteorological Experiment (BOMEX; Siebesma *et al.*, 2003), Atmospheric Radiation Measurement (ARM; Brown *et al.*, 2002), and the Atlantic Tradewind Experiment (ATEX; Stevens *et al.*, 2001), has shown that modern LES is capable of accurately simulating cumulus cloud dynamics and resolving the intricacies of entrainment processes, even down to non-trivial geometrical properties of the cloud edge (Siebesma and Jonker, 2000).

Before lateral mixing can be studied in LES, one first has to define the cloud and environment (the so-called sampling method). Often applied is cloud-core sampling where all LES grid points that contain liquid water ($q_l > 0$) and are positively buoyant ($\theta_v > \overline{\theta_v}$) are considered to be part of the cloudy updraught. Here q_l is the liquid water content, θ_v is the virtual potential temperature (being a measure of density) and $\overline{\theta_v}$ is the slab-averaged virtual potential temperature.

In the 1990s, computer resources were too limited to perform LES of deep convection. However, early LES results provided important insight into shallow convection including lateral mixing. For example, Siebesma and Cuijpers (1995) showed in a careful analysis of LES results that the turbulent transport can be accurately described with a bulk mass flux approach, especially when the cloud-core sampling method is applied. So diagnosing ε and δ in this way from LES gives a strong guideline to the ε and δ that should be used in a NWP or climate model bulk mass flux scheme. Therefore, LES provides a powerful tool to study the qualitative and quantitative behaviour of the lateral mixing coefficients. For example, Siebesma and Cuijpers (1995) found that the typical entrainment/detrainment values for shallow convection usually applied at that time were an order of magnitude too small. Several LES studies of shallow convection also revealed that the detrainment varies much more than the entrainment and therefore has a much larger impact on variations in the mass flux profile (de Rooy and Siebesma, 2008). A more theoretical basis for this was given by de Rooy and Siebesma (2010), who showed that a significant part of the variations in δ is associated with the cloud-layer depth. This LES finding is applied in the convection parametrisation schemes of de Rooy and Siebesma (2008) and Neggers (2009) (section 4.2). LES studies further revealed the influence of environmental humidity conditions (e.g. Derbyshire *et al.*, 2004) and the properties of the updraught itself (e.g. de Rooy and Siebesma, 2008) on the mass flux profiles.

LES studies have also been utilised to investigate lateral mixing in a more fundamental way. For example, Heus and Jonker (2008) and Jonker *et al.* (2008) described the influence of a subsiding shell on lateral mixing (section 3.8). Further, Heus *et al.* (2008) convincingly showed that lateral mixing is responsible for diluting the cloudy updraught and not cloud-top mixing, as was thought for a long time (Squires, 1958; Paluch, 1979, and sections 2.5, 3.7). LES studies like Zhao and Austin (2005b) investigated the mixing between clouds and their environment during the life cycle of single clouds. Finally, two recent LES studies derived more direct, locally evaluated entrainment and detrainment coefficients (Romps, 2010; Dawe and Austin, 2011b, and section 3.6). Whereas Dawe and Austin (2011b) accomplished this by carefully determining the net velocity through the cloud environment interface, Romps (2010) used an inventive definition of entrainment and detrainment. Compared to LES results diagnosed within the bulk mass flux framework, both latter studies diagnosed significantly larger lateral mixing coefficients. This discrepancy can be explained by the fact that the lateral transport in Romps (2010) and Dawe and Austin (2011b) involves smaller differences between cloud and environment properties.

Due to increased computer resources, LES models are now capable of simulating deep convection (e.g. Kuang and Bretherton, 2006; Khairoutdinov and Randall, 2006; Khairoutdinov *et al.*, 2009). Such LES studies turned out to be very insightful. A complicating factor is the important role of the microphysics on cloud dynamics which still needs to be parametrised in LES of deep convection.

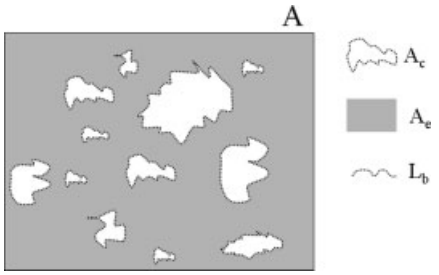

Figure 1. Schematic diagram showing an ensemble of clouds at a certain height. A_c, A_e and A represent the cloudy area (white), the environmental area (grey), and the total horizontal domain ($= A_c + A_e$), respectively. The interface between the cloudy area and the environment is plotted as a dashed line and has a total length L_b (adapted from de Rooy and Siebesma, 2010).

3. New insights in entrainment and detrainment processes

3.1. Introduction

So far, in our historical review we have been rather vague on the precise definition of the entrainment and the detrainment processes. The purpose of this section is to make a more precise notion of these mixing processes and to explore their behaviour in a more fundamental way. First we will provide basic definitions of the entrainment and detrainment processes. We will proceed to apply these first to a rising dry plume which is governed by a purely entrainment process. Subsequently, entrainment and detrainment will be reviewed in the context of the steady state cloud model of Asai and Kasahara (1967), which will make the notion of organised versus turbulent entrainment and detrainment more precise. We will proceed by reviewing the various ways of determining the exchange rates from LES. Finally LES results are used to discuss the long-lasting controversy between the relative importance of lateral versus vertical mixing in cumulus convection, and the importance of the vicinity of the cloud in the lateral mixing process.

3.2. General definitions

Basic definitions are introduced here following Siebesma (1998). A convenient starting point is the conservation law of a scalar variable ϕ

$$\frac{\partial \phi}{\partial t} + \nabla \cdot \mathbf{v}\phi = F, \tag{4}$$

where $\mathbf{v}$ denotes the three-dimensional velocity vector and where all possible sources and sinks of ϕ are collected in F. For the sake of simplicity, we assume a Boussinesq flow, implying that the density in (4) is constant and has been divided out. We consider a domain with a horizontal area A and we are interested in the lateral mixing between a cloudy area A_c and a complementary environmental area A_e at a given height z such as is sketched schematically in Figure 1.

At this point, we do not need to be more specific on the precise definition of the cloudy area, but it should be noted that it may consist of many different 'blobs' (or clouds) that can change in shape and size as a function of time and height. By integrating (4) horizontally over the cloudy area $A_c(z, t)$, applying the Leibniz integral rule and the Gauss divergence theorem, a transparent conservation equation of the cloudy

area for ϕ can be deduced (Siebesma, 1998),

$$\frac{\partial a_c \phi_c}{\partial t} + \frac{1}{A}\oint_{\text{interface}} \widehat{\mathbf{n}}\cdot(\mathbf{u}-\mathbf{u}_i)\phi \,\mathrm{d}l + \frac{\partial a_c \overline{w\phi}^c}{\partial z} = a_c F_c, \quad (5)$$

where $a_c = A_c/A$ is the fractional cloud cover, $\widehat{\mathbf{n}}$ is an outward-pointing unit vector perpendicular to the interface, $\mathbf{u}$ is the full 3D velocity vector at the interface, and $\mathbf{u}_i$ is the velocity of the interface. Overbars and variables with subscript c denote averages over the cloudy part. In the special case $\phi = 1$ and $F_c = 0$, we recover the continuity equation

$$\frac{\partial a_c}{\partial t} + \frac{1}{A}\oint_{\text{interface}} \widehat{\mathbf{n}}\cdot(\mathbf{u}-\mathbf{u}_i)\,\mathrm{d}l + \frac{\partial a_c w_c}{\partial z} = 0. \quad (6)$$

Equation (6) has a simple geometrical interpretation. The net change of the cloud fraction is a result of the net lateral inflow of mass across the cloudy interface on the one hand and the vertical mass flux divergence on the other hand. Let us emphasize that it is the mass velocity $\mathbf{u}$ *relative* to the interface velocity $\mathbf{u}_i$ that enters in the interface term. This way it is guaranteed that there is no net inflow if a cloud is simply advected by the mean wind. Since entrainment is usually associated with the inflow of mass into the cloudy area, whereas detrainment with the complementary outflow, it seems natural to define these processes as

$$\left.\begin{aligned} E &= -\frac{1}{A}\oint_{\widehat{\mathbf{n}}\cdot(\mathbf{u}-\mathbf{u}_i)<0} \widehat{\mathbf{n}}\cdot(\mathbf{u}-\mathbf{u}_i)\,\mathrm{d}l, \\ D &= \frac{1}{A}\oint_{\widehat{\mathbf{n}}\cdot(\mathbf{u}-\mathbf{u}_i)>0} \widehat{\mathbf{n}}\cdot(\mathbf{u}-\mathbf{u}_i)\,\mathrm{d}l, \end{aligned}\right\} \quad (7)$$

so that, realizing that $E \equiv \epsilon M$ and $D \equiv \delta M$, (6) reduces under steady state conditions to

$$\frac{1}{M}\frac{\partial M}{\partial z} = \varepsilon - \delta. \quad (8)$$

Although it is relative straightforward to determine $E - D$ as a residual from (6), it is by no means trivial to determine entrainment and detrainment rates separately, either in laboratory experiments or in numerical simulations. We will come back to this point in subsection 3.6.

3.3. Dry plumes

While entrainment and detrainment are easily defined mathematically, the physical processes involved are not always fully understood and in fact can depend on how we define the interface across which the mixing processes are defined. Buoyant dry plumes, which rise in a non-turbulent environment, provide a relatively simple example. They entrain environmental air and show virtually no detrainment. Such plumes rise and grow almost indefinitely, until they are diluted to the extent that they are absorbed in the chaos of molecular motions. If we denote the length of the perimeter of the plume by L_b, define u_b as the net mean velocity at the boundary of the plume,

$$\overline{u}^b \equiv u_b \equiv \frac{1}{L_b}\oint_{\text{interface}} \widehat{\mathbf{n}}\cdot(\mathbf{u}-\mathbf{u}_i)\,\mathrm{d}l \quad (9)$$

and assume steady state and a circular geometry, i.e. $A_c = \pi R^2$ and $L_b = 2\pi R$, it is straightforward to rewrite (6) as

$$\frac{1}{M}\frac{\partial M}{\partial z} = \frac{L_b}{A_c}\frac{u_b}{w_c} \simeq \frac{1}{R}\frac{2u_b}{w_c}. \quad (10)$$

which provides a justification for the famous entrainment relationship for plumes (Morton *et al.*, 1956) and a physical interpretation of the proportionality constant in (1).

3.4. Steady-state single cloud

However, atmospheric clouds differ from dry plumes. Entrainment of unsaturated environmental air leads to the evaporation of cloud liquid water. Some cloud parcels will lose their buoyancy and ultimately their liquid water and are then by definition detrained. This naturally requires the inclusion of the detrainment process. It is not possible to make more precise statements on the entrainment and detrainment processes unless we are more specific about the physics that play a role in these processes. A popular model has been proposed by Asai and Kasahara (1967), in which a steady state cloud is assumed to be cylinder-shaped with a radius R. Further, they presume a scale separation between turbulent exchange across the cloud interface and a larger scale in- or outflow resulting from the buoyancy-driven mass flux convergence or divergence inside the cloud. This is done by applying a Reynolds decomposition of the flux across the cloud boundary for thermodynamic conserved variables ϕ:

$$\overline{u\phi}^b \equiv u_b\phi_b + \overline{u'\phi'}^b, \quad (11)$$

in which by convention u_b is positive if it is pointing out of the cloud, and the mean property of ϕ along the cloud boundaries, ϕ_b, is defined as

$$\overline{\phi}^b \equiv \phi_b \equiv \frac{1}{L_b}\oint_{\text{interface}} \phi \,\mathrm{d}l\,. \quad (12)$$

This scale separation allows the introduction of turbulent entrainment and detrainment on the one hand, and organised entrainment driven by convergence and organised detrainment driven by divergence on the other hand. More specifically if, following Asai and Kasahara (1967), we approximate the turbulent flux by an eddy diffusivity approach and make an upwind approximation of the organised in- and outflow (i.e. $\phi_b = \phi_c$ if $u_b > 0$, and $\phi_b = \phi_e$ if $u_b < 0$), one can derive for the various terms on the RHS of (3):

$$\varepsilon_{\text{turb}} = \delta_{\text{turb}} = \frac{2\eta}{R}, \quad (13)$$

$$\varepsilon_{\text{dyn}} = H(-u_b)\frac{1}{w_c}\frac{\partial w_c}{\partial z}, \quad (14)$$

$$\delta_{\text{dyn}} = -H(u_b)\frac{1}{w_c}\frac{\partial w_c}{\partial z}, \quad (15)$$

where H denotes the Heaviside function, w_c is the average vertical velocity in the cloud, and η is a dimensionless constant analogous with the constant of proportionality between horizontal (here radial) and vertical velocity fluctuations in the mixing length theory, which is of the order

$O(1)$. If these results are coupled to updraught equations for temperature, moisture and vertical velocity and fed with the proper boundary conditions at cloud base, one typically finds net condensational heating in the lower part of the cloud that feeds the buoyancy leading to an acceleration of the updraught. This acceleration has a negative feedback since it will induce an inflow due to the organised entrainment that will eventually slow down the updraught, leading to divergence and an organised detrainment in the upper part of the cloud. A few remarks should be made. First the fact that the turbulent mixing is assumed to be symmetric in terms of an equal entrainment and detrainment has been criticised by Randall and Huffman (1982). In their model, the interface is defined as the boundary of the mass of turbulent air associated with the cloud. Therefore they model the turbulent mixing solemnly as a entrainment process and not as a turbulent mixing process as in Asai and Kasahara (1967). Secondly the form of the organised entrainment and detrainment is a direct result of the strong assumption that the cloud has a constant radius R. With w_c predicted by an updraught equation, ε_{dyn} and δ_{dyn} are determined by (14) and (15). Therefore the constant R assumption can be seen as the organised entrainment and detrainment closure of the Asai and Kasahara model. If the interface is defined as the buoyant part of the cloud, a thermodynamic constraint should determine how R varies with height. The buoyancy sorting principle put forward by Kain and Fritsch (1990) is a step in that direction. In their model (section 4.1), equal masses of environmental and cloudy air are assumed to form various mixtures. It is then assumed that negatively buoyant mixtures are detrained whereas positive buoyant mixtures are entrained. However in that case the closure problem is shifted to the choice of how much mass is available for supplying such mixtures and which probability distribution function to choose for the occurrence of the various mixtures. Another interesting idea is put forward by Neggers (2009). In their approach, a probability function of temperature and moisture within the cloud is reconstructed from different updraughts. Such a joint pdf allows the determination of the area of the cloud that is positively buoyant, and hence the variation of its radius as a function of height.

3.5. *Determination of entrainment and detrainment from LES: Bulk estimates*

LES have been proven to be an extremely useful tool in determining entrainment and detrainment rates in cumulus clouds, initially for shallow cumulus (e.g. Siebesma and Cuijpers, 1995; Siebesma *et al.*, 2003), but more recently also for deep convection (e.g. Kuang and Bretherton, 2006; Khairoutdinov *et al.*, 2009). These studies have provided useful guidance for parametrisations of detrainment and entrainment in large-scale models (e.g. de Rooy and Siebesma, 2010; Siebesma and Holtslag, 1996; Gregory, 2001). The traditional way to diagnose E and D is not through the direct use of (7), but rather through an effective bulk entrainment and detrainment rate defined as

$$\left.\begin{aligned} E_\phi &\equiv -\frac{1}{A\phi_e}\oint_{\widehat{\mathbf{n}}\cdot(\mathbf{u}-\mathbf{u}_i)<0} \widehat{\mathbf{n}}\cdot(\mathbf{u}-\mathbf{u}_i)\phi \,\mathrm{d}l,\\ D_\phi &\equiv \frac{1}{A\phi_c}\oint_{\widehat{\mathbf{n}}\cdot(\mathbf{u}-\mathbf{u}_i)>0} \widehat{\mathbf{n}}\cdot(\mathbf{u}-\mathbf{u}_i)\phi \,\mathrm{d}l, \end{aligned}\right\} \tag{16}$$

where we have indexed the exchange rates E_ϕ and D_ϕ to indicate that there might be a ϕ dependence. Substituting these definitions in (5) then directly gives

$$\frac{\partial a_c\phi_c}{\partial t} = M(\varepsilon_\phi\phi_e - \delta_\phi\phi_c) - \frac{\partial a_c\overline{w\phi}^c}{\partial z} + a_cF_c. \tag{17}$$

By combining (17) and (8), the bulk fractional entrainment and detrainment rates can be diagnosed from LES output. For this diagnosis the subplume term in $\overline{w\phi}^c$ is usually ignored, steady state is assumed and, if we consider a conserved variable, the source term F_c is zero, so that the entrainment can be diagnosed according to Betts (1975):

$$\frac{\partial\phi_c}{\partial z} = -\varepsilon(\phi_c - \phi_e). \tag{18}$$

Most importantly, the exchange rates deduced in this way are used in a similar way in parametrisations. Indeed, virtually all parametrisations use (17) as a starting point and therefore need to be fed by the same effective bulk entrainment rates that are diagnosed in this way by LES. The price to be paid is that the bulk exchange rates ε_ϕ and δ_ϕ are now no longer necessarily a property of the turbulent flow, but can be dependent on the field ϕ (cf. Yano *et al.*, 2004).

3.6. *Determination of entrainment and detrainment from LES: Direct estimates*

The use of the 'true' exchange rates as defined by (7) is far from trivial from a numerical point of view, mainly because it was until recently unclear how to diagnose the local velocity $\mathbf{u}_i$ of the interface. While in reality $\mathbf{u}$ and $\mathbf{u}_i$ are of the same order of magnitude, the cloudy surface in an LES model shifts one grid box in one time step, giving rise to very high unrealistic $\mathbf{u}_i$ values. However, two recent independent studies (Romps, 2010; Dawe and Austin, 2011b) have been able to tackle this problem and derive E and D directly based on (7). Dawe and Austin (2011b) follow a straightforward method by applying a subgrid interpolation to determine the position of the cloud surface more accurately. Romps (2010) follows a different approach; instead of a bulk cloud sampling, Romps defines a local activity operator, $\mathcal{A}$, which is 1 if q_l and w_c exceed some threshold value. The local entrainment rate, E is then the local rate at which air flips from inactive to active and vice versa for the detrainment rate, D. Subsequently, Romps (2010) diagnoses E and D as

$$E = \max\left\{0, \frac{\partial}{\partial t}(\rho\mathcal{A}) + \nabla\cdot(\rho\mathbf{u}\mathcal{A})\right\}, \tag{19}$$

$$D = \max\left\{0, -\frac{\partial}{\partial t}(\rho\mathcal{A}) - \nabla\cdot(\rho\mathbf{u}\mathcal{A})\right\}, \tag{20}$$

where $\partial(\rho\mathcal{A})/\partial t + \nabla\cdot(\rho\mathbf{u}\mathcal{A})$ is referred to as 'activity source', built up by the motion of the cloud surface (first term) and air advection into or out of the cloud (second term). Summing this 'activity source' over the complete period the grid cell is adjacent to the cloud surface can be seen as an implicit subgrid interpolation of the cloud surface and it also ensures that a purely advective cloud has $E = D = 0$.

As Romps (2010) and Dawe and Austin (2011b) evaluate E and D locally, there are some important differences with the bulk approach. For example, bulk estimates of ε and δ are

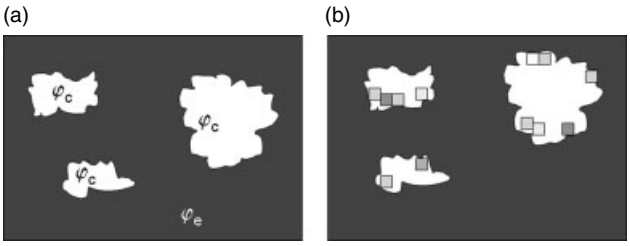

Figure 2. Schematic diagram showing the situation relevant for (a) detrainment in a bulk mass flux scheme, and (b) directly measured detrainment (Romps, 2010). In (a), detraining cloudy air always has the average properties of the cloudy area, ϕ_c. In (b), the detraining gridboxes are represented by the squares and, as indicated by the grey scale, the detraining air has properties between the average cloudy and environmental air.

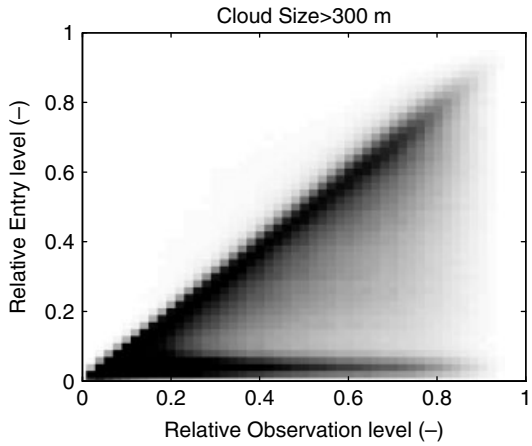

Figure 3. The relative height at which particles entered the cloud as a function of relative observation level, for all clouds in the ensemble with a vertical size large than 300 m (reproduced from Heus *et al.*, 2008).

tracer dependent, whereas direct measurements of the lateral mixing coefficients are only related to the local properties of the flow (Romps, 2010). However, the most striking result was that the bulk plume approach underestimates entrainment and detrainment by roughly a factor of 2 (Romps, 2010). This is elucidated in Figure 2(a) showing the conceptual picture following the bulk concept. The air that detrains from the cloud is supposed to have the same property as air averaged over all clouds ($\phi_{\text{detraining air}} = \overline{\phi}^{c} \equiv \phi_c$). Figure 2(b) illustrates the situation in the Romps (2010) local approach. Some gridboxes are diagnosed as detraining according to the direct measurement technique, here presented by grey squares. In general, the relatively less buoyant cloudy grid boxes will detrain. Possibly a grid box that has just entrained will now detrain again. Consequently, the potential temperature of the detraining grid boxes will on average be lower than the potential temperature averaged over the complete cloudy area. Similarly, it will normally not be the most humid grid boxes that detrain. So detraining air will on average have properties between the average cloudy and average environmental air. The same arguments hold for entrainment. Because the difference between detraining and environmental air or entraining and cloudy air is larger in the bulk approach than in the Romps framework, the corresponding ε and δ values should be smaller in the bulk approach to get the same correct lateral fluxes. Very recently, this discrepancy between bulk and directly measured ε and δ values has been further investigated and quantitatively explained by Dawe and Austin (2011a).

A potentially important result of Romps (2010) and Dawe and Austin (2011b) is the change of the cloud properties due to detrainment, because in their approach detraining air does not have the average cloud properties (Figure 2). This is in contrast with the entraining plume model of Betts (1975) (Eq. 18) used in the bulk mass flux concept, where only ε determines the dilution. On the other hand, if ε is diagnosed in LES within the bulk framework, it will describe the correct cloud dilution as long as it is applied in a bulk scheme. One might say that this diagnosed bulk ε implicitly takes into account the negative dilution due to detrainment.

Direct entrainment and detrainment calculations are very useful to understand the underlying processes. At the same time, we should realize that ultimately the different approaches lead to the same correct dilution of the cloud properties and turbulent transport, as long as the mixing coefficients are diagnosed and applied in the same framework. Therefore, bulk diagnosed entrainment and detrainment values are appropriate for usage in a model bulk mass flux parametrisation.

3.7. *On the origin of entrained air in cumulus clouds*

The controversy between lateral and vertical mixing, discussed in section 2.5, was recently studied in more detail within the framework of LES. Interestingly the LES study by Heus *et al.* (2008), which in many ways can be regarded as a follow-up of the study by Lin and Arakawa (1997), does reproduce the Paluch mixing lines, but *refutes* the conclusion implied by the diagram. They reached this conclusion by using a large number of Lagrangian particles which could be traced back in time so as to reveal the true origin of the entrained air. The technique makes it possible to obtain a wealth of statistical data by analysing all clouds in the ensemble and additionally averaging in time, and revealed the precise fraction of particles that entered near the top of the cloud, the fraction of particles that entered the lateral edge of the cloud, and the fraction that entered via the cloud base. Figure 3, reproduced from the original paper, shows a density plot of the relative entry level (height of first entry of a particle in the cloud normalised by cloud size) and the (relative) level of observation in the cloud. The horizontal dark-gray band is indicative of the particles that entered via cloud base. The dark diagonal band is indicative of particles entering via the lateral edge near the observation level. The light grey lower right triangle shows the fraction of particles that were laterally entrained at levels below the observation level. However, in the light of the present discussion, the most important feature of Figure 3 is the white upper-left triangle representing in a statistical sense the striking absence of particles entrained from the top. If cloud-top entrainment, followed by penetrative downdraughts, were to be a significant mechanism, then this upper-left triangle should have been filled to a reasonable extent; clearly it is not. The question is still open why cloud data points tend to line up in a Paluch diagram the way they do, thus providing *compelling but flawed* support for the importance of cloud-top entrainment for cumulus dynamics. Heus *et al.* (2008) found some evidence for the buoyancy sorting mechanism suggested by Taylor and Baker (1991), but actually not enough to serve as a full explanation. Such deeper understanding of Paluch diagrams, which seems to require further research, might provide crucial 'convergence' of the cloud community with respect to the dominant entrainment mechanism in cumulus convection.

3.8. *Relevance of the near vicinity of clouds*

From the premise that lateral entrainment is important, it follows that the immediate vicinity of clouds must be important as well because it defines the properties of the air to be entrained into the cloud. Observational studies by, for example, Jonas (1990), Rodts *et al.* (2003) and more recently by Wang *et al.* (2009) and Heus *et al.* (2009a), reveal how the (thermo)dynamic and microphysical properties of the near-cloud environment differ significantly from the environmental properties further away from the cloud. Studying individual cloud transects, Jonas (1990) noted the presence of a thin shell of subsiding air surrounding clouds and pointed out the importance of it for understanding the droplet spectrum in clouds, taking into account that the shell in principle could contain air with cloud-top properties. As to the cause of the descending shell, Jonas (1990) identified two mechanisms, mechanical forcing and evaporative cooling resulting from mixing saturated and unsaturated air at the cloud edge. As a follow-up, Rodts *et al.* (2003) studied a large number of horizontal cloud transects measured during the Small Cumulus Microphysics Study (SCMS; Knight and Miller, 1998), and created a statistical average by normalizing each transect by the corresponding cloud width. They confirmed the persistent occurrence of the descending shell of air surrounding the cloud and found their data to be most consistent with the mechanism of evaporative cooling.

Detailed LES by Heus and Jonker (2008) of the SCMS and BOMEX cases reproduced the existence of the descending shell in the simulations and, based on a budget analysis of vertical momentum in the model, negative buoyancy resulting from evaporative cooling was identified as the main driver for the downward motion. Since the shell surrounds clouds along their entire perimeter –which can be substantial due to its geometrical properties (Lovejoy, 1982; Siebesma and Jonker, 2000) –Jonker *et al.* (2008) used LES to precisely quantify the total downward mass flux through the shell. To this end, they analysed the data conditioned on the distance to the (nearest) cloud edge. Rather surprisingly, the total downward mass flux in the cloud shells was found to compensate virtually all the total upward mass flux of the cloud field, not so much due to the negative velocity in the shell (which is rather modest compared to the upward velocity in the cloud core), but rather due to the large area that is associated with the cloud-edge region. This view was confirmed in an observational study by Heus *et al.* (2009a), who analysed RICO (Rain in Cumulus over the Ocean) data, adopting the strategy of conditionally averaging quantities with respect to the distance to the cloud edge.

One implication of the large downward mass flux in the vicinity of clouds is that the total downward mass flux in the environment distant from the clouds must be quite small. As shown by Verzijlbergh *et al.* (2009), this in turn has a tremendous effect on the efficacy of vertical transport of species in the regions away from clouds, because the up- and downward transport in the cumulus layer takes place only where clouds are located (which is usually only a small fraction of space). Apart from the dynamical aspects, the microphysical structure of the cloud-edge region is also of fundamental interest; Wang *et al.* (2009) describe a recent observational study.

4. Entrainment and detrainment in mass flux parametrisations

For almost all NWP and climate models, convection is still a subgrid process which thus has to be parametrised. One of the key questions is how the parametrisation should account for the influence of environmental conditions (e.g. relative humidity). As will become clear in this section, a wide variety of approaches exist. In convection parametrisations, a distinction is usually made between shallow and deep convection. We will start with developments mainly concerning shallow convection (sections 4.1 and 4.2), followed by section 4.3 dealing with differences between shallow and deep convection. Sections 4.4 and 4.5 are relevant for both shallow and deep convection.

4.1. *Kain–Fritsch type buoyancy sorting schemes and updates*

Convection schemes including the parametrisations of ε and δ show a large variety of complexity. On one hand of the spectrum are the simple bulk mass flux schemes with constant ε and δ values whose values are loosely based on (1). However it has been shown that such simple fixed values for the mixing coefficients are too limited since their values appear to be dependent on cloud-layer depth (de Rooy and Siebesma, 2008) and on the environmental conditions (e.g. Kain and Fritsch, 1990; Derbyshire *et al.*, 2004). To take the environmental conditions into account, Raymond and Blyth (1986) and Kain and Fritsch (1990) introduced the buoyancy sorting concept. These widely applied schemes, together with some recent updates, are described here.

Although not specifically designed for shallow convection, the parametrisation of Kain and Fritsch (1990) is widely applied as such. In their approach, different mixtures of in-cloud and environmental air are made. Negatively buoyant mixtures are assumed to detrain whereas positively buoyant mixtures entrain. Due to evaporative cooling, θ_v of the mixture can drop below that of the environment, so leading to detrainment. This process is illustrated in Figure 4 which shows the θ_v of a mixture of cloudy air with a fraction χ of environmental air. For example, purely cloudy air has $\chi = 0$ and obviously $\theta_v(\chi = 0) = \theta_{v,c}$. The critical

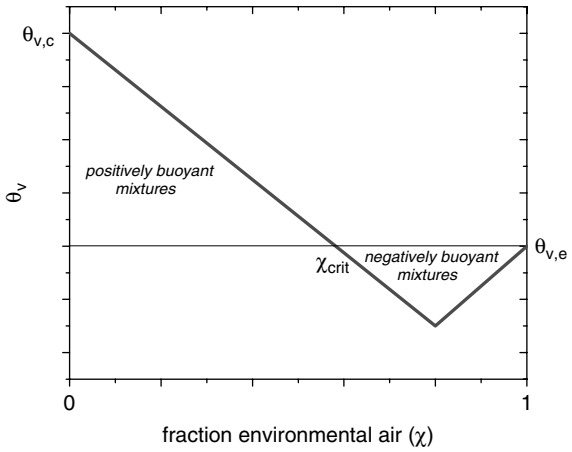

Figure 4. The virtual potential temperature of a mixture of cloudy air with environmental air as a function of the fraction, χ, of environmental air. The virtual potential temperatures of the cloudy and environmental air are θ_{vc} and θ_{ve}, respectively. χ_{crit} is the fraction environmental air necessary to make the cloudy air just neutrally buoyant.

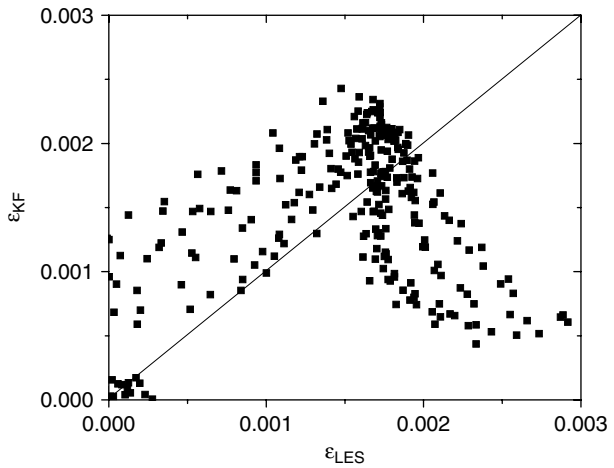

Figure 5. Fractional entrainment rates as diagnosed (using the core sampling) from LES, ε_{LES}, versus estimates from (21) with $\varepsilon_0 = 0.02$ (optimal value), ε_{KF}. These results are for the BOMEX case (Siebesma *et al.*, 2003).

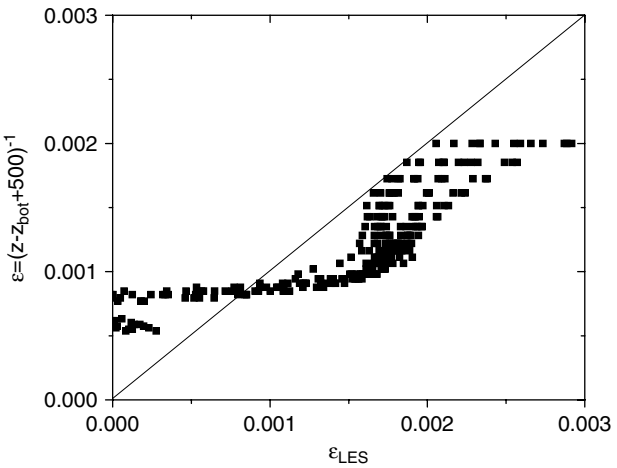

Figure 6. As Figure 5, but with estimates from $\varepsilon = (z - z_{bot} + 500)^{-1}$, where z is the height (m) and z_{bot} is cloud-base height.

fraction χ_{crit} is defined as the fraction of environmental air needed to make the mixture just neutrally buoyant. In the original Kain–Fritsch (KF) scheme, mixtures with $\chi < \chi_{crit}$ are assumed to entrain while mixtures with $\chi > \chi_{crit}$ are assumed to detrain.

To derive the fractional entrainment and detrainment coefficients within the KF concept, the amount of mass used for mixing (not discussed), as well as the pdf for the occurrence of the various mixtures has to be determined. As there is no *a priori* knowledge on which pdf should be chosen, it is natural to assume that all mixtures have an equal probability of occurence, which leads to (Bretherton *et al.*, 2004)

$$\varepsilon_{KF} = \varepsilon_0 \chi_{crit}^2, \tag{21}$$

$$\delta_{KF} = \varepsilon_0 (1 - \chi_{crit})^2, \tag{22}$$

where ε_0 is the fractional mixing rate, i.e. the fractional mass available for mixing, which in the original KF concept is kept constant. We have used LES results from a shallow cumulus convection case based on observations made during BOMEX (Holland, 1972) in order to evaluate ε based on (21), and compared these with LES diagnosed values based on (18). Even if we choose a best estimate of ε_0, Figure 5 shows a low correlation. Better results can be obtained if ε is estimated by a simple decreasing function with height (Figure 6).

When the original KF concept was used in practice, several deficiencies were reported, many of them related to the corresponding lateral mixing coefficients. These deficiencies, including some modifications to address them, are well summarised by Kain (2004). In parallel, variations on KF schemes were developed, such as that by Bretherton *et al.* (2004). Kain (2004) pointed out that, according to (21), dry conditions (corresponding to small χ_{crit}) will result in small ε values and consequently little dilution of the updraught. Hence, the original KF concept can lead to the contra-intuitive result of deeper cloud layers in combination with drier (more hostile) environmental conditions. This behaviour of the KF model was also confirmed by Jonker (2005). In contrast, LES results show considerably shallower cloud depths for drier environmental conditions (Derbyshire *et al.*, 2004). To fix the above-mentioned deficiency, some of the newer versions of the KF scheme prescribe a lower limit to the entrainment of 50% of the environmental air involved in the mixing process and/or try to use state-dependent values for ε_0.

Another deficiency, this time related to (22) and discussed by Bretherton *et al.* (2004), is the excessive detrainment if all negatively buoyant mixtures are rejected from the updraught. Bretherton *et al.* (2004) dealt with this problem by introducing a length-scale below which negatively buoyant parcels can maintain upward velocity and consequently do not detrain yet.

4.2. *Parametrising the shape of the shallow mass flux profile*

From the discussion in the previous subsection, it can be concluded that, although the KF concept contains interesting and important ideas, there are some fundamental problems. In practice these problems are solved by rather drastic modifications and tuning parameters which more or less undermine the physical attractiveness of the concept. In this subsection, two recent alternative shallow convection parametrisations (de Rooy and Siebesma, 2008; Neggers, 2009) are described that make use of χ_{crit}, an important parameter originally applied in buoyancy sorting schemes (see the previous section). More importantly, these parametrisations distinguish themselves from other mass flux schemes because the entrainment and the shape of the mass flux profile are treated separately. In such a framework, ε can be dedicated to an adequate description of the change of the cloud properties with height (via (18)) and therewith the cloudy updraught termination height, without being used for the mass flux profile (via (8)). In this way, several problems with conventional convection schemes can be circumvented.

As convincingly argued later, the separate treatment of ε and the mass flux profile is based on the much larger variation of δ in comparison with ε and therewith its much larger impact on variations in the mass flux profile. This is incompatible with the KF concept because if we use ε_{KF} and δ_{KF} ((21) and (22)), these coefficients vary in a similar but opposite way to χ_{crit}^2 only and therefore have a similar impact on variations in the mass flux profile related to variations in χ_{crit}^2. However, as first pinpointed by de Rooy and Siebesma (2008), the variations from case to case and hour to hour observed in mass flux profiles can be almost

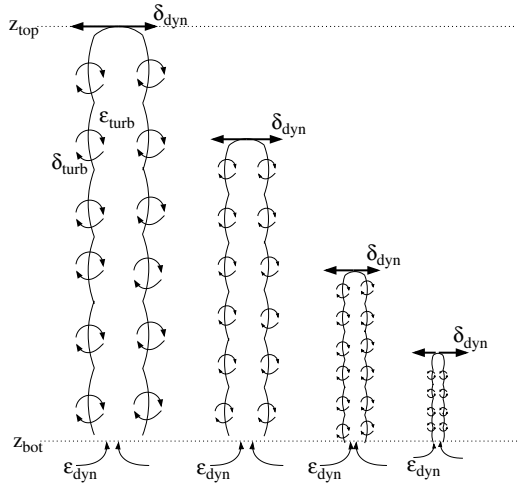

Figure 7. Schematic diagram of a shallow convection cloud ensemble with massive entrainment, $\varepsilon_{\rm dyn}$, at cloud base, $z_{\rm bot}$, and massive detrainment, $\delta_{\rm dyn}$, at the top of individual clouds. From cloud base to the top of individual clouds, turbulent lateral mixing takes place, presented by $\varepsilon_{\rm turb}$ and $\delta_{\rm turb}$. For individual clouds, the mass flux is constant with height. The deepest cloud reaches height $z_{\rm top}$, the top of the cloud layer. This picture is valid for divergent conditions, i.e. $\partial M/\partial z < 0$, which is usually the case for shallow convection.

exclusively related to the fractional detrainment. Numerous LES studies support this by revealing order-of-magnitude larger variations from case to case and hour to hour in δ than in ε (e.g. Figure 8; Jonker *et al.*, 2006; Derbyshire *et al.*, 2011). Nevertheless, its implication for parametrising convection is almost never used or even discussed.

Apart from this empirical evidence, de Rooy and Siebesma (2010) also provided a sound theoretical bases for the observed large variation in δ and the strong coupling to variations in the mass flux profile. Based on a general total water specific humidity budget equation and within the usually applied bulk mass flux framework, they derived a general picture for a shallow convection cloud ensemble as shown in Figure 7. As in Asai and Kasahara (1967), a distinction is made between small-scale diffusive turbulent lateral mixing, expressed by $\varepsilon_{\rm turb}$ and $\delta_{\rm turb}$ and larger-scale advective transport across the lateral boundaries, described by $\varepsilon_{\rm dyn}$ and $\delta_{\rm dyn}$ (also section 2). Figure 7 is in line with Arakawa and Schubert (1974), but now also includes a turbulent detrainment term which counteracts $\varepsilon_{\rm turb}$, leading to a constant mass flux of individual clouds until the massive detrainment at their top. As a result of different cloud sizes in the ensemble, the massive detrainment of the various clouds shows up as a dynamical detrainment term throughout the cloud layer. Figure 7 reveals that it is mainly the dynamical detrainment that regulates the shape of the cloud layer mass flux profile. Indeed, de Rooy and Siebesma (2010) showed that the vertical structure of the mass flux is largely determined by the detrainment while the detrainment is determined by the vertical structure of the cloud fraction, all in agreement with the conceptual picture sketched in Figure 7. Accepting that the shape of the detrainment is determined by the mass flux, and assuming a monotonic decrease of the mass flux from cloudbase height $z_{\rm bot}$ to cloud-top height $z_{\rm top}$ gives an zeroth-order estimate of the detrainment of

$$\delta \sim \frac{1}{M}\frac{\partial M}{\partial z} \sim \frac{1}{z_{\rm top} - z_{\rm bot}}. \qquad (23)$$

This equation also illustrates the cloud-layer depth dependence of δ, first mentioned by de Rooy and Siebesma (2008) and clearly recognisable in several LES studies (e.g. Figure 8; Jonker *et al.*, 2006).

The above-mentioned empirical and theoretical arguments support the approach of de Rooy and Siebesma (2008) to describe variations in the non-dimensionalised mass flux profile with a detrainment coefficient. Their flexible δ ensures a certain mass flux profile. So in principle the mass flux profile itself is parametrised in their approach and therewith the concept of δ becomes obsolete. Note that the cloud-layer height dependence is taken care of by evaluating and prescribing the mass flux with a non-dimensionalised height and mass flux.

In de Rooy and Siebesma (2008), it is also shown that variations in δ, and therewith the mass flux profile, depend not only on cloud depth (23) but also on the environmental conditions such as the vertical stability and the relative humidity. These dependencies are well described by $\chi_{\rm crit}$ which can be written approximately as (de Rooy and Siebesma, 2008)

$$\chi_{\rm crit} = \frac{c_p \pi}{L}\frac{\delta\theta_v}{q_s(\beta-\alpha)(1-RH) - \alpha q_{l,u}}, \qquad (24)$$

where c_p denotes the specific heat, L the latent heat, π the Exner function, $\delta\theta_{\rm v}$ the difference in virtual potential temperature between cloudy updraught and environment, RH the relative humidity of the environment, $q_{\rm l,u}$ the liquid water in the cloudy updraught, and α and β are constants. Note that $\chi_{\rm crit}$ increases both with the buoyancy of the cloudy updraught and with the environmental relative humidity. LES results show that detrainment rates decrease with increasing values of $\chi_{\rm crit}$. This relation can be easily understood from physical considerations. Small $\chi_{\rm crit}$ values correspond to marginally buoyant, often relatively small, clouds rising in a dry, hostile environment (section 4.1). It is likely (and confirmed by LES) that under such conditions the mass flux will decrease rapidly (large detrainment). The opposite is true for large buoyant clouds rising in a friendly, humid environment, corresponding to large $\chi_{\rm crit}$ values (small detrainment). Via this $\chi_{\rm crit}$ dependence, δ and the mass flux profile are varying not only with the RH of the environment, but also with the properties (buoyancy) of the updraught itself. de Rooy and Siebesma (2008) provide further details.

Instead of the critical mixing fraction, Neggers (2009) uses a moist zero buoyancy deficit, $q_{\rm t}^x - \overline{q_{\rm t}}$ where, $q_{\rm t}^x$ is the total water specific humidity at mixing fraction $\chi_{\rm crit}$. Note that the moist zero buoyancy deficit is proportional to $\chi_{\rm crit}$. By using this moist zero buoyancy deficit to estimate the cloud fraction and therewith also the cloudy updraught velocity (via the pdf of $w_{\rm c}$), Neggers (2009) establish a link between the mass flux and statistical cloud schemes (also section 3.4).

In line with the arguments mentioned in this subsection, an adaptive detrainment parametrization has been proposed very recently by Derbyshire *et al.* (2011). LES results in their study (their Figures 5 and 6) confirm that δ varies much more strongly with environmental RH than ε.

4.3. *Differences between deep and shallow convection*

Besides varying with the environmental conditions, entrainment and detrainment rates may vary considerably between

shallow and deep convection. Figure 8 shows as an example profiles of ε and δ derived from LES. Here ε and δ are computed from (8) and (18) with $\phi = s$ where s is the frozen moist static energy (e.g. Bretherton *et al.*, 2005),

$$s = c_p T + gz + L\, r_\mathrm{v} - L_\mathrm{f}\, r_\mathrm{i}\,, \tag{25}$$

where r_v is the water vapour mixing ratio, L_f is the latent heat of freezing and r_i is the mixing ratio of ice. Figures 8(a, b) are based on LES simulations conducted for the Kwajalein Experiment (KWAJEX) over the West Pacific warm pool for the period 23 July to 4 September 1999. The entrainment and detrainment rates are stratified and averaged as a function of cloud depth. Figures 8(c, d) contain the results for midlatitude continental convection, whereby the LES were driven by measurements made at the ARM Southern Great Plains station between 18 June and 3 July 1997. Due to the large variability in synoptic conditions and consequently in entrainment and detrainment rates, only specific times are shown in Figures 8(c, d). The time spans from 0900 to 1700 local time (LT) on 27 June 1997 and encompasses a typical diurnal cycle of surface-forced convection, from shallow (0900 LT) to deep convection with maximum precipitation at 1700 LT.

Figure 8 clearly indicates that the transition from shallow to deep convection is accompanied by a reduction in entrainment and detrainment rates. This is true both for tropical oceanic (Figures 8(a, b)) as well as midlatitude continental (Figures 8(c, d)) convection. Similar reductions in ε have been noticed by DelGenio and Wu (2010) for TWP-ICE (Tropical Warm Pool International Cloud Experiment), Kuang and Bretherton (2006) for an idealised oceanic transition case, and Khairoutdinov and Randall (2006) for the LBA (Large-scale Biosphere–Atmosphere) experiment over Amazonia. The variations in δ appear also much larger than the ε changes in Figure 8. de Rooy and Siebesma (2008) have already pinpointed the importance of the detrainment rate and its cloud depth dependence (clearly visible in Figures 8(b, d)) in controlling the mass flux profile (section 4.2). Apart from this, other effects are thought to be responsible for reducing ε and δ. Firstly, detrainment of former clouds moistens the environment; the entrained air becomes moister, the evaporative cooling due to the mixing of cloudy and environmental air is reduced, and consequently the detrainment will decrease (e.g. de Rooy and Siebesma, 2008). However the effect on ε seems less clear. As described in section 4.4, Bechtold *et al.* (2008) apply an entrainment rate which decreases with increasing RH of the environment. This explicit dependency on RH has a large beneficial effect in the general circulation model of the European Centre for Medium-range Weather Forecasts (ECMWF). On the other hand, in the widely applied scheme of Kain and Fritsch (1990), ε (21) increases with increasing RH of the environment. So the influence of environmental RH on ε is yet far from established.

Secondly, several studies (e.g. Kuang and Bretherton, 2006; Khairoutdinov and Randall, 2006; Khairoutdinov *et al.*, 2009) have suggested that the formation of cold pools plays a key role in the transition from shallow to deep convection. In particular, the formation of cold pools yields larger clouds which entrain less and thus are more suitable to reach greater depth. Recent attempts to unify shallow and deep convective parametrisations have therefore added explicit relations to tighten their entrainment and detrainment rates to precipitation or its evaporation, as a measure of cold pool activity (Hohenegger and Bretherton, 2011; Mapes and Neale, 2011). Without such explicit relations, deep convection schemes tend to trigger deep convection too early; this is the cause of many operational NWP and climate models predicting precipitation systematically too early in the diurnal cycle over land in the Tropics (Betts and Jakob, 2002).

4.4. *RH-dependent entrainment*

A possible approach to account for the influence of environmental conditions on convection is to use an entrainment explicitly depending on RH. Here an example is presented together with some alternative entrainment formulations.

The sensitivity of moist convection with respect to environmental moisture gained considerable attention since the work by Derbyshire *et al.* (2004) who set up a series of single-column models (SCMs) and cloud-resolving models (CRMs) where the atmosphere is relaxed to different values of the ambient RH. The convection schemes employed in their SCMs were not able to match the sensitivity of the mass flux profiles with respect to environmental RH as represented by the CRMs.

Motivated by their study and observations that mid-tropospheric humidity modulates tropical convection (Redelsperger *et al.*, 2002), Bechtold *et al.* (2008) revised the ECMWF convection scheme, including an entrainment formulation that explicitly accounts for RH dependency. It was shown that the revised convection scheme also greatly improves midlatitude and tropical variability in the ECMWF model on various scales including the representation of wavenumbers 1 and 2 Madden–Julian Oscillation (MJO) (Madden and Julian, 1971). Also recently, several CRM studies and model developments (e.g. DelGenio and Wu, 2010; Chikira and Sugiyama, 2010; Kim and Kang, 2011) focused on state-dependent entrainment rates, their sensitivity to environmental profiles, and their impact on the large-scale circulation and variability.

On the basis of the Derbyshire *et al.* (2004) model set-up, we discuss some necessary ingredients for a bulk entrainment model in order to represent the sensitivity of the mass flux profiles with respect to environmental RH.

The model set-up simply consists of running the ECMWF SCM for a 24 h period while relaxing the free atmosphere (above 2 km) humidity fields to specified values of 25, 50, 70, and 90% RH while the background boundary-layer moisture profile is identical for all runs.

Different updraught entrainment formulations are evaluated. The base version is a formulation that has evolved from Bechtold *et al.* (2008) and constitutes the ECMWF operational formulation since 2010:

$$\left.\begin{aligned} \varepsilon &= \varepsilon_0\{1.3 - RH(z)\} f_\mathrm{scale}\,, \\ \text{with } \varepsilon_0 &= 1.8 \times 10^{-3}\mathrm{m}^{-1}, \\ \text{and } f_\mathrm{scale} &= \left\{\frac{q_\mathrm{sat}(z)}{q_\mathrm{sat}(\mathrm{z_{bot}})}\right\}^3, \end{aligned}\right\} \tag{26}$$

where ε depends for each height z on the RH and a scaling function f_scale which is a polynomial function of the ratio of the saturation specific humidities q_sat at level z and at convective cloud base $\mathrm{z_{bot}}$. The scaling function aims to mimic the effect of an ensemble of clouds. Furthermore,

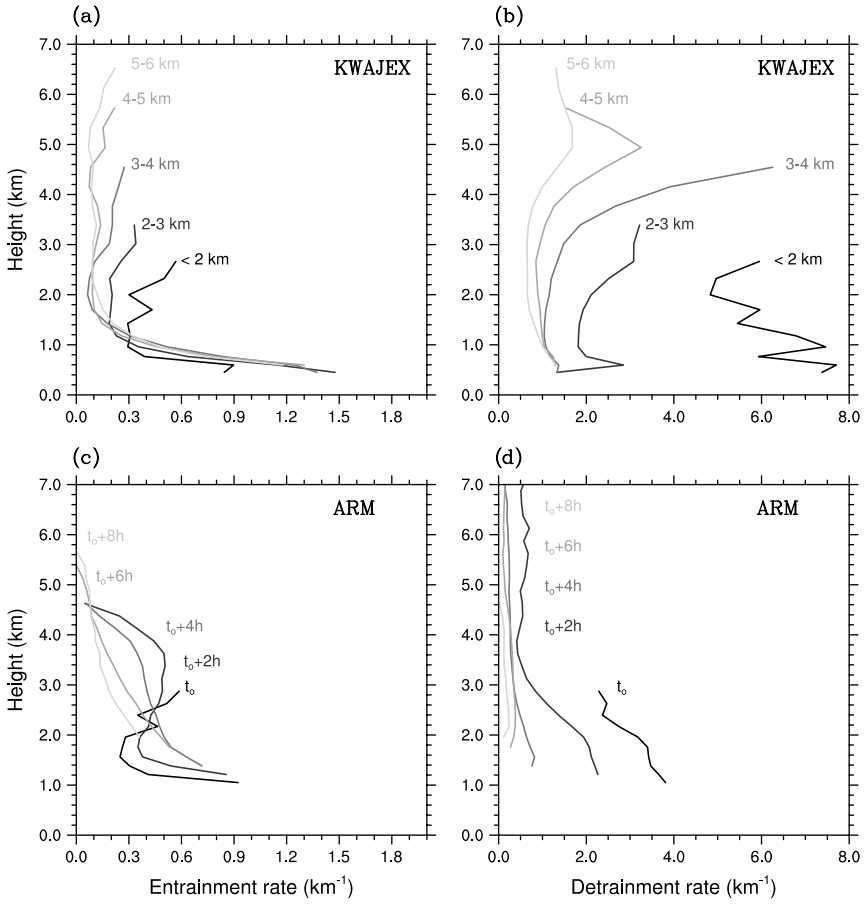

Figure 8. Profiles of (a, c) fractional entrainment and (b, d) detrainment rates based on LES of the (a, b) KWAJEX and (c, d) ARM cases. (a) and (b) show entrainment and detrainment rates averaged for clouds of various depths (i.e. < 2 km, 2–3, 3–4, 4–5 and 5–6 km). (c) and (d) show entrainment and detrainment rates at 2 h time intervals with t_o corresponding to 0900 LT on 27 June 1997.

entrainment is only applied when the buoyancy of the updraught is positive and the distinction between deep and shallow convection is made by multiplying the entrainment rates in (26) by a factor of two if the cloud thickness of a test parcel is smaller than 200 hPa. Figure 9 shows the entrainment profiles with (26) for the different RH regimes in Derbyshire *et al.* (2004). LES results presented by Derbyshire *et al.* (2011) (Figure 5) for the same RH regimes also reveal increasing ε values with decreasing RH in the lower part of the cloud layer.

Fractional detrainment rates are parametrised differently, namely as the sum of a vertically constant turbulent detrainment and a term that is proportional to the decrease in updraught kinetic energy when the buoyancy is negative (Bechtold *et al.*, 2008). The turbulent detrainment rate for deep convection is set to $\delta_{\text{turb}} = 0.75 \times 10^{-4}\text{m}^{-1}$, whereas for shallow convection it is equal to the entrainment rates (in accordance with de Rooy and Siebesma, 2010, Figure 7). This simple detrainment formulation together with the entrainment rate that strongly decreases with height assures a convective mass flux profile that from a certain level can decrease with height even for positively buoyant convection throughout.

A comparison between the operational ECMWF SCM version using (26) and CRM data is shown in Figures 10(a, g). As an example, we also illustrate the data from the Met Office model that was one of the two participating CRMs in Derbyshire *et al.* (2004). (The CRM data had been scaled by a factor of 0.6 as the mass flux scaling between the

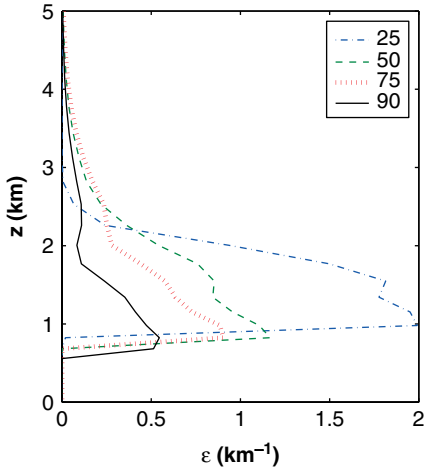

Figure 9. Entrainment profiles using (26) for background RH of 25% (dash-dotted), 50% (dashed), 70% (dotted) and 90% (solid). This figure is available in colour online at wileyonlinelibrary.com/journal/qj

participating SCM and CRMs varied by a factor 0.5–1.5.) Comparing also to the other SCM and CRM results in Derbyshire *et al.* (2004), the current results suggest that the model is broadly able to represent the increase of the cloud height and amplitude of the mass flux with increasing RH, and in particular the shallow convection regime for the 25% RH profile. The cloud-top heights for the deep regimes are lower in the ECMWF model than in the CRM, but global

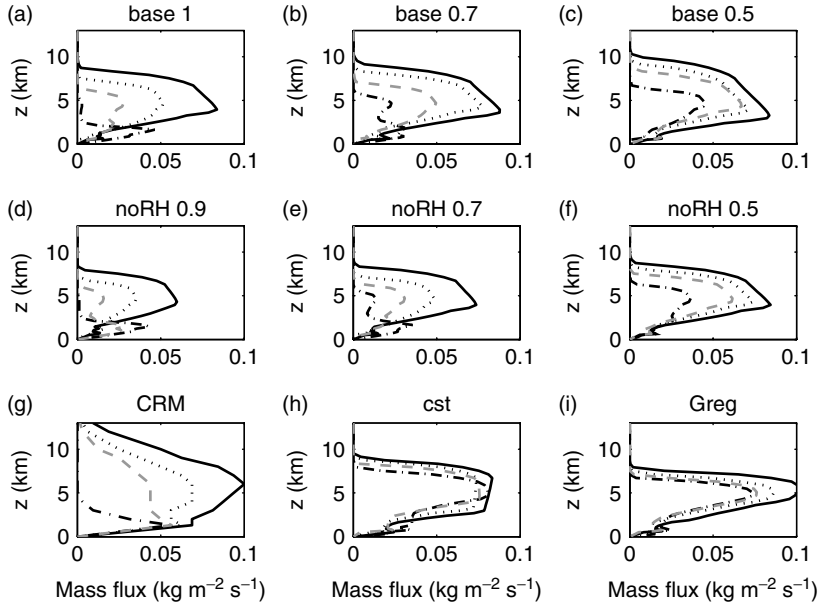

Figure 10. Time- and/or domain-averaged convective mass flux profiles for background RH of 25% (dash-dotted), 50% (dashed grey), 70% (dotted) and 90% (solid) as obtained from ECMWF SCM simulations with different entrainment formulations and CRM simulations. (a)–(c) are with entrainment according to (26) with scale factors of 1, 0.7,and 0.5; (d)–(f) are with entrainment (26) without relative humidity dependence and scale factors of 0.9, 0.7 and 0.5; (g) is for Met Office CRM data scaled by a factor of 0.6; (h) is for constant entrainment; and (i) is for entrainment formulation by Gregory (2001).

model evaluation versus satellite observations (not shown) suggest realistic cloud-top heights in the ECMWF model (Ahlgrimm *et al.*, 2009; Ahlgrimm and Forbes, 2012).

Next, sensitivity studies to the entrainment profile are performed including a series of variations to (26). In the first series, entrainment (26) is decreased by factors of 0.7 and 0.5. The corresponding results in Figure 10(b, c) show that as a consequence the cloud-top heights generally rise and the shallow convection regime transits to a congestus regime compared to the base version (Figure 10(a)), but still a distinct sensitivity to the RH remains.

In the second series of sensitivity experiments, (26) is simplified by dropping the RH-dependent term,

$$\varepsilon_{\mathrm{noRH}} = \beta \varepsilon_0 f_{\mathrm{scale}} \tag{27}$$

and by applying different scaling factors $\beta = 0.9, 0.7$ and 0.5. The corresponding results in Figure 10(d–f) appear rather similar to the base version (Figure 10(a–c)), but the mass flux amplitudes are smaller and there is less sensitivity to the cloud-top heights between the different scaling factors.

Simplifying even further, the vertical scaling function is also dropped to obtain a vertical constant entrainment rate $\varepsilon_{\mathrm{const}} = \beta \varepsilon_0$. Choosing $\beta = 0.05$ in Figure 10(h), one notices immediately the lack of RH sensitivity. This is due to the low entrainment rate, but this low value is necessary in order to produce reasonable cloud-top heights for the deep convection regimes.

Finally, we apply the entrainment formulation suggested by Gregory (2001), which has also been advocated by DelGenio and Wu (2010) and Chikira and Sugiyama (2010),

$$\varepsilon_{\mathrm{Greg}} = \beta B w_{\mathrm{c}}^{-2}; \qquad B = g \frac{\Delta T_{\mathrm{v}}}{T_{\mathrm{v}}}, \tag{28}$$

where B is the buoyancy, g is gravity, T_{v} and ΔT_{v} are the virtual temperature and the cloudy updraught virtual temperature excess, respectively. The corresponding results in Figure 10(i) have been obtained using β values close to the literature, i.e. $\beta = 0.03$ for deep convection and $\beta = 0.06$ for shallow convection. Note that, based on LES diagnoses, de Rooy and Siebesma (2010) found a much larger optimal value, $\beta = 0.12$ for (28), which will increase the sensitivity to RH but also leads to lower cloud tops. Figure 10(i) suggests that (28) does not provide sufficient sensitivity in terms of cloud-top height, and also in terms of the shape of the mass flux profiles. To remedy the characteristic top-heavy mass flux profiles inherent to this formulation, a detrainment formulation might be required which is different from the present ECMWF one. Finally, we have also tested an entrainment formulation of the type $\varepsilon_z = \beta z^{-1}$, but the results (not shown) for this case were similar to the Gregory formulation.

The conclusions that can be retained from this SCM study is that a bulk mass flux formulation can broadly reproduce the sensitivity of convection to the mid-tropospheric moisture field. However, this requires strong entrainment rates of $\mathrm{O}(10^{-3})$ in the lower troposphere. The results also suggest that the entrainment rates should strongly decrease with height, in order to control the mass flux profile, and also to allow for strong values near the cloud base, and that the inclusion of a further explicit dependence of the entrainment rate on RH leads to further more realistic sensitivities to the large-scale moisture fields. As suggested in section 4.2, an alternative approach is to parametrise the entrainment and the mass flux profile independently, thus providing the flexibility to simultaneously obtain correct cloud-top heights, sensitivity to the environment, and mass flux profiles.

Interestingly, DelGenio and Wu (2010), using CRM data on diurnal cycle convection, confirmed the order of magnitude of the entrainment rates used here in the ECMWF base version. As a general remark, we finally mention that a SCM study can never replace a study in a global model since it can only span a very small parameter space of atmospheric conditions and cannot reproduce the interaction between

convection and the large scale. Also, the influence of the entrainment and the precise shape of the mass flux profile on the momentum transport and the wind field cannot be adequately modelled in a SCM.

4.5. *Stochastic entrainment*

A key issue in modern research in cumulus convection pertains to the variability among convecting elements. It is not yet clear if most of this variability can be attributed to variability in the thermodynamic properties close to cloud base, or if variability in the entrainment process above cloud base also plays a fundamental role. Recent LES studies (Romps and Kuang, 2010b) and SCM simulations (Sušelj *et al.*, 2011) have highlighted the important role of stochastic entrainment in producing realistic thermodynamic structures for a variety of shallow convection case-studies.

Lateral entrainment is essential to represent the interaction between updraughts and the surrounding environment. Although numerous entrainment formulations have been developed, as is amply described in this review article, the problem of parametrising lateral entrainment in moist convection is still not solved. The parametrisation of Neggers *et al.* (2002) partially tackles the issue of producing a realistic amount of variability between updraughts. In this formulation, the entrainment rate is inversely proportional to the product of the updraught vertical velocity and a (constant) time-scale. In this way, the positive feedback between the updraught vertical velocity and the entrainment rate effectively increases the variability between updraughts. One of the key problems with this type of parametrisation is that the results are quite sensitive to the value of the time-scale.

An alternative perspective of lateral entrainment is provided by authors such as Raymond and Blyth (1986) and Romps and Kuang (2010a,b), who suggested that entrainment should be represented as a stochastic process. In Sušelj *et al.* (2011), an entrainment parametrisation similar to the one suggested by the LES studies of Romps and Kuang (2010b) was implemented in a SCM. It was essentially assumed that most entrainment occurs as discreet events. In practice, the simplest form for an entrainment event is assumed: when the updraught grows a distance dz, the probability of entrainment is dz/L_0, where L_0 represents a mean distance the updraught needs to grow to entrain once. The entrainment coefficient can be determined stochastically from a Bernoulli distribution and along the finite length z the probability of an entrainment event follows a Poisson distribution.

With this entrainment parametrisation, two stochastic processes are driving the moist updraught properties: the stochastic initialization of the moist updraughts at cloud base and the stochastic entrainment rate. The results of Sušelj *et al.* (2011) suggest that using only these two important and independent stochastic mechanisms, realistic thermodynamic structures can be simulated for a variety of shallow cumulus events.

5. Conclusions and discussion

Over the last 15 years we have witnessed a renaissance of entrainment and detrainment studies, mainly due to the fact that LES have become an extremely useful tool for diagnosing these mixing processes. This has resulted in new insights as well as improved parametrisations for entrainment and detrainment in operational NWP and climate models.

A number of these new insights have been reviewed in this article. Firstly, on the origin of entrained air, different theories have coexisted for several decades. The prevailing opinion has shifted from lateral entrainment (starting with Stommel, 1947) to cloud top entrainment (starting with Squires, 1958) as the main mechanism. However, detailed particle tracking studies in LES have shown unambiguously (section 3.7) that cloud-top entrainment plays no significant role in the mixing process compared to lateral mixing.

From the premise that entrainment involves lateral movements, the vicinity of clouds is important since it defines the properties of the entraining air. Observational evidence (e.g. Jonas, 1990; Rodts *et al.*, 2003) as well as an LES study (Heus and Jonker, 2008) reveal the existence of a descending shell with properties significantly different from the average environment (section 3.8).

A slightly related topic can be found in the articles of Romps (2010) and Dawe and Austin (2011b) (section 3.6). Although their methods are different, both articles present methods for directly determining entrainment and detrainment rates from the basic definitions (7) rather than by using the approximate bulk method (16). The direct determined exchange rates are a factor of two larger than the ones diagnosed using the bulk approach. As elucidated in section 3.6 and explained in detail by Dawe and Austin (2011b), this is due to the fact that the direct method involves air with properties near the interface of interest, while the bulk method is based on air with mean properties of the environment and the cloud. Consequently, larger ε and δ values are necessary to get the same lateral mixing flux as in the bulk approach. Accordingly, ε and δ are smaller in the bulk approach. An advantage of the directly determined entrainment and detrainment rates is that they are properties of the turbulent flow, and not dependent on the used variable in the flow, as is the case of the bulk derived properties. Does that imply that parametrisations should strive to reproduce the direct entrainment and etrainment rates? The answer is firmly no. Parametrisations should use those LES-diagnosed rates that are compatible with their updraught model. For instance, if a parametrisation is using a simple entraining plume model like (18), then such a parametrisation should employ bulk entrainment and detrainment rates as diagnosed by LES using the same simplified equation. The reason for this is simply that such entrainment and detrainment rates provide the optimal turbulent fluxes, which is the prime objective of any convection parametrisation.

From the many LES studies on entrainment and detrainment in (mainly) shallow cumulus convection over the last ten years, a physically consistent picture of the cloud dynamics and mixing is emerging (de Rooy and Siebesma, 2010) (Figure 7). Cumulus convection is constituted by an ensemble of cumulus clouds, many small and shallow ones and fewer larger and deeper ones. They all share the same cloud-base height, but have different cloud-top heights. The main inflow occurs at cloud base and can be intepreted as organised entrainment. All clouds are diluted through equal turbulent entrainment and detrainment, but the smaller clouds are exposed to larger rates than the larger clouds, simply due to dimensional surface to volume ratio. Organised detrainment takes place at the cloud top and therefore it is the cloud size distribution,

or more precisely the closely related cloud-top height distribution, which determines the shape of the mass flux profile of the whole cloud ensemble. This can be affected by external factors such as the atmospheric stability or free tropospheric relative humidity. Higher relative humidity and/or decreasing atmospheric stability supports more relatively deep clouds, shifting the organised detrainment to higher altitudes, and leading to a slower decrease of the mass flux with height.

What are the consequences for shallow cumulus parametrisations? For bulk parametrisations one should use entrainment parametrisations that decrease with height. This reflects the fact that, near cloud base, the 'bulk' entrainment is dominated by the many small clouds, while higher in the cloud layer, the entrainment is smaller since it is dominated by the larger clouds. The organised detrainment can vary strongly from case to case and is therefore the key process that determines the shape of the mass flux profile (de Rooy and Siebesma, 2008, 2010). Fortunately, the detrainment appears to be well correlated to χ_{crit} (section 4.2) which can be determined by using a simple entraining plume model. Alternatively, one can use χ_{crit} to directly parametrise the mass flux (de Rooy and Siebesma, 2008) or the cloud core fraction (Neggers, 2009). In the latter case, the mass flux profile can be constructed by combining it with the vertical velocity equation which is routinely used in the entraining plume model.

Instead of a bulk model, one can also employ a multiplume model such as pioneered by Arakawa and Schubert (1974). In that case, closure assumptions on the shape of the cloud size distribution is required. Such a parametrisation is computationally more expensive as it requires several plume updraughts. On the other hand, it is potentially conceptually simpler since many of the assumptions that need to enter into a bulk parametrisation are not necessary anymore as they are sorted out by the various plumes explicitly.

At this point it is not completely clear to what extent these conclusions which mainly apply to shallow convection also apply to deep convection, but preliminary studies reveal that the overall picture remains the same. For example, for deep convection the detrainment as well as the mass flux profile appear to be well correlated to χ_{crit}. Nevertheless, deep convection results in additional complications which need to be parametrised. Most importantly, precipitation triggers downdraughts that promote the formation of cold pools. The mesoscale organisation associated with the cold pools supports deep convection and accelerates the transition from shallow to deep convection (Böing *et al.*, 2012). Attempts are being made to include this process by adding explicit relations to tighten ε and δ to precipitation or its evaporation (section 4.3; Hohenegger and Bretherton, 2011; Mapes and Neale, 2011).

Based on these increased physical insights on entrainment and detrainment, one might expect to observe some convergence of cumulus parametrisations in operational weather and climate models. However, an extensive variety of parametrisations has been developed for ε and δ without a sign of any convergence towards certain approaches. Moreover, there is no consensus about the necessary dependencies included in the formulations of the mixing coefficients. A remarkable example is the dependency of the entrainment on relative humidity. In two recent and operationally applied approaches by Kain and Fritsch (1990) and Bechtold *et al.* (2008) (cf. sections 4.1, 4.4), this dependency is simply inverse.

What are possible causes of the non-converging developments? Most importantly, many parametrisations are still developed without a direct comparison of the formulations against LES-diagnosed ε and δ (e.g. Kain and Fritsch, 1990, and Figure 5). Yet LES experiments deliver an excellent opportunity to validate potential expressions within the corresponding model framework. One obvious example that LES results are simply ignored by developers is the large observed variation from case to case and hour to hour in δ, even by orders of magnitude. Apart from the strong empirical evidence, these large variations have also been recently explained from theoretical considerations (de Rooy and Siebesma, 2010). Variations in δ can be related to different environmental conditions, such as relative humidity and stability. However, the largest variations in δ are often related to variations in the cloud-layer depth (de Rooy and Siebesma, 2008), as can be observed e.g. during daytime convection over land with a deepening cloud layer. To the knowledge of the authors, only two shallow convection parametrisation schemes capture these large variations in δ, namely those by de Rooy and Siebesma (2008) and Neggers (2009) (section 4.2).

Another reason for the lack of convergence is that the development and the actual implementation of parametrisation is a slow process. This is partly due to the relatively small number of scientists who are working directly on the development and implementation of convection parametrisations. At the same time, it is becoming increasingly difficult to implement new parametrisation schemes that demonstrate immediate increase of skill, since operational models are highly optimised and contain compensating biased errors. Therefore, reducing one bias through implementing an improved parametrisation often results in a deteriorating model skill, and retuning or removing a compensating bias becomes necessary. This requires a thorough knowledge of many of the relevant parametrised processes and obviously slows down the process of model improvement through parametrisation development. Because of this increasing complexity, we recommend that parametrisations should be kept as simple as possible. That is, one should try to capture only the most substantial processes responsible for (LES-)observed variations in lateral mixing.

Finally, we want to mention a study of Mironov (2009) (extending the work of de Roode *et al.*, 2000), in which analogies between mass flux and Reynolds-averaged equations reveal that entrainment and detrainment have to describe a wide variety of processes that depend on the mean flow variables in different ways. Consequently, the use of ε and δ in a mass flux framework might be troublesome.

Randall *et al.* (2003) confirmed the slow progress on the parametrisation of convection. They therefore advocated the use of superparametrisation through the use of two-dimensional CRM within each grid box of weather and climate models to break what they called the cloud parametrisation deadlock. Although this is an interesting option, we here suggest a less radical approach. In order to speed up progress in parametrising lateral mixing in cumulus convection, we advocate a stronger and more systematic use of LES results and coordinated intercomparison studies on the basis of observations and LES results. This pathway has been taken by the Global Energy and Water cycle Experiment

(GEWEX) Cloud System Studies (GCSS) and will be continued by the Global Atmospheric System Studies (GASS) Panel. Also it is important to have continous interactions and discussions between the various research communities, as in the COST ES0905 project (http://convection.zmaw.de), to facilitate further convergence and progress in this area.

Finally, we are entering an new era in which high-resolution models ($\sim$ 1–10 km) become operational as NWP models (e.g. Staniforth and Wood, 2008; Weisman, 2008; Baldauf *et al.*, 2011; Seity *et al.*, 2011). At these resolutions, cumulus convection is partly resolved but still needs partial parametrisations. In this so-called grey zone, many assumptions that are common at coarser resolutions break down: quasi-equilibrium no longer holds, the cloud-core fraction is no longer much smaller than unity and smaller grid boxes cannot contain a representative cumulus ensemble. This requires a more stochastic and scale-adaptive approach. But even for these high-resolution models, we believe that entrainment and detrainment processes will remain vital for parametrisation and a valuable research topic for years to come.

Acknowledgements

Helpful discussions with Kees Kok and Stephan de Roode are greatly appreciated. We thank Peter Blossey for having performed some of the LES shown in this study. We would also like to thank two anonymous reviewers and the associate editor for their useful comments. This study was initiated and partially supported by the European Commission through the COST Action ES0905.

References

Ahlgrimm M, Forbes RM. 2012. The impact of low clouds on surface short-wave radiation in the ECMWF model. *Mon. Weather Rev.* submitted.

Ahlgrimm M, Randall D, Köhler M. 2009. Evaluating cloud frequency of occurence and top height using space-borne lidar observations. *Mon. Weather Rev.* **137**: 4225–4237.

Arakawa A, Schubert WH. 1974. Interaction of a cumulus cloud ensemble with the large-scale environment, Part I. *J. Atmos. Sci.* **31**: 674–701.

Asai T, Kasahara A. 1967. A theoretical study of the compensating downward motions associated with cumulus clouds. *J. Atmos. Sci.* **24**: 487–496.

Baldauf M, Seifert A, Förstner J, Majewski D, Raschendorfer M, Reinhardt T. 2011. Operational convective-scale numerical weather prediction with the COSMO model: description and sensitivities. *Mon. Weather Rev.* **139**: 3887–3905.

Bechtold P, Kohler M, Jung T, Doblas-Reyes F, Leutbecher M, Rodwell M, Vitart F, Balsamo G. 2008. Advances in simulating atmospheric variability with the ECMWF model: From synoptic to decadal time-scales. *Q. J. R. Meteorol. Soc.* **134**: 1337–1351.

Betts AK. 1975. Parametric interpretation of trade-wind cumulus budget studies. *J. Atmos. Sci.* **32**: 1934–1945.

Betts AK. 1982. Saturation point analysis of moist convective overturning. *J. Atmos. Sci.* **39**: 1484–1505.

Betts AK. 1985. Mixing-line analysis of clouds and cloudy boundary layers. *J. Atmos. Sci.* **42**: 2751–2763.

Betts AK, Jakob C. 2002. Study of diurnal cycle of convective precipitation over Amazonia using a single-column model. *J. Geophys. Res.* **107**: 4732–4745.

Boatman JF, Auer AH. 1983. The role of cloud-top entrainment in cumulus clouds. *J. Atmos. Sci.* **40**: 1517–1534.

Böing SJ, Jonker HJJ, Siebesma AP, Grabowski WW. 2012. Influence of the subcloud layer on the development of a deep convective ensemble. *J. Atmos. Sci.* DOI: 10.1175/JAS-D-11-0317.1.

Bretherton CS, McCaa JR, Grenier H. 2004. A new parameterization for shallow cumulus convection and its application to marine subtropical cloud-topped boundary layers. Part I: Description and 1D results. *Mon. Weather Rev.* **132**: 864–882.

Bretherton CS, Blossey PN, Khairoutdinov M. 2005. An energy-balance analysis of deep convective self-aggregation above uniform SST. *J. Atmos. Sci.* **62**: 4273–4292.

Brown AR, Cederwall RT, Chlond A, Duynkerke PG, Golaz J-C, Khairoutdinov JM, Lewellen DC, Lock AP, Macvean MK, Moeng C-H, Neggers RAJ, Siebesma AP, Stevens B. 2002. Large-eddy simulation of the diurnal cycle of shallow cumulus convection over land. *Q. J. R. Meteorol. Soc.* **128**: 1075–1094.

Chikira M, Sugiyama M. 2010. A cumulus parameterization with state-dependent entrainment rate. Part I: Description and sensitivity to temperature and humidity profiles. *J. Atmos. Sci.* **67**: 2171–2193.

Dawe JT, Austin PH. 2011a. The influence of the cloud shell on tracer budget measurements of LES cloud entrainment. *J. Atmos. Sci.* **68**: 2209–2920.

Dawe JT, Austin PH. 2011b. Interpolation of LES cloud surfaces for use in direct calculations of entrainment and detrainment. *Mon. Weather Rev.* **139**: 444–456.

DelGenio AD, Wu J. 2010. Sensitivity of moist convection to environmental humidity. *J. Climate* **23**: 2722–2738.

Derbyshire SH, Beau I, Bechtold P, Grandpeix J-Y, Piriou J-M, Redelsperger J-L, Soares PMM. 2004. Sensitivity of moist convection to environmental humidity. *Q. J. R. Meteorol. Soc.* **130**: 3055–3079.

Derbyshire SH, Maidens AV, Milton SF, Stratton RA, Willett MR. 2011. Adaptive detrainment in a convective parametrization. *Q. J. R. Meteorol. Soc.* **137**: 1856–1871.

de Roode SR, Duynkerke PG, Siebesma AP. 2000. Analogies between mass-flux and Reynolds-averaged equations. *J. Atmos. Sci.* **57**: 1585–1598.

de Rooy WC, Siebesma AP. 2008. A simple parameterization for detrainment in shallow cumulus. *Mon. Weather Rev.* **136**: 560–576.

de Rooy WC, Siebesma AP. 2010. Analytical expressions for entrainment and detrainment in cumulus convection. *Q. J. R. Meteorol. Soc.* **136**: 1216–1227.

Gregory D. 2001. Estimation of entrainment rate in simple models of convective clouds. *Q. J. R. Meteorol. Soc.* **127**: 53–72.

Gregory D, Rowntree PR. 1990. A mass flux convection scheme with representation of cloud ensemble characteristics and stability-dependent closure. *Mon. Weather Rev.* **118**: 1483–1506.

Heus T, Jonker HJJ. 2008. Subsiding shells around shallow cumulus clouds. *J. Atmos. Sci.* **65**: 1003–1018.

Heus T, van Dijk G, Jonker HJJ, van den Akker HEA. 2008. Mixing in shallow cumulus clouds studied by Lagrangian particle tracking. *J. Atmos. Sci.* **65**: 2581–2597.

Heus T, Jonker HJJ, van den Akker HEA, Griffith EJ, Koutek M, Post FH. 2009a. A statistical approach to the life cycle analysis of cumulus clouds selected in a vitual reality environment. *J. Geophys. Res.* **114**: D06208, DOI: 10.1029/2008JD010917.

Heus T, Pols CFJ, Jonker HJJ, van den Akker HEA, Lenschow DH. 2009b. Observational validation of the compensating mass flux through the shell around cumulus clouds. *Q. J. R. Meteorol. Soc.* **135**: 101–112.

Hohenegger C, Bretherton CS. 2011. Simulating deep convection with a shallow convection scheme. *Atmos. Chem. Phys.* **11**: 10389–10406.

Holland JZ. 1972. Comparative evaluation of some BOMEX measurements of sea surface evaporation, energy flux and stress. *J. Phys. Oceanogr.* **2**: 476–486.

Houghton H, Cramer H. 1951. A theory of entrainment in convective currents. *J. Meteorol.* **8**: 95–102.

Jensen JB, Austin PH, Baker MB, Blyth AM. 1985. Turbulent mixing, spectral evolution and dynamics in a warm cumulus cloud. *J. Atmos. Sci.* **42**: 173–192.

Jonas PR. 1990. Observations of cumulus cloud entrainment. *Atmos. Res.* **25**: 105–127. DOI: 10.1016/0169-8095(90)90008-Z.

Jonker S. 2005. 'Evaluation study of the Kain–Fritsch convection scheme'. Technical report TR275. KNMI: De Bilt, The Netherlands.

Jonker HJJ, Verzijlbergh RA, Heus T, Siebesma AP. 2006. 'The influence of the sub-cloud moisture field on cloud size distributions and the consequences for entrainment'. Extended abstract in *Proceedings of 17th Symposium on Boundary Layers and Turbulence*, San

Diego, USA. Amer. Meteorol. Soc: Boston, USA. Available at http://ams.confex.com/ams/pdfpapers/111021.pdf

Jonker HJJ, Heus T, Sullivan PP. 2008. A refined view of vertical mass transport by cumulus convection. *J. Geophys. Res.* **35**: L07810, DOI: 10.1029/2007GL032606.

Kain JS. 2004. The Kain–Fritsch convective parameterization: An update. *J. Appl. Meteorol.* **43**: 170–181.

Kain JS, Fritsch JM. 1990. A one-dimensional entraining/detraining plume model and its application in convective parameterization. *J. Atmos. Sci.* **47**: 2784–2802.

Kain JS, Fritsch JM. 1993. Convective parameterization for mesoscale models. The Kain–Fritsch scheme. *Meteorol. Monographs* **24**: 165–170.

Khairoutdinov MF, Randall D. 2006. High-resolution simulation of shallow to deep convection transition over land. *J. Atmos. Sci.* **63**: 3421–3436.

Khairoutdinov MF, Krueger SK, Moeng C-H, Bogenschutz PA, Randall D. 2009. Large-eddy simulation of maritime deep tropical convection. *J. Adv. Model Earth Syst.* **1**: Art. 15, DOI: 10.3894/JAMES.2009.1.15.

Kim D, Kang I-S. 2011. A bulk mass flux convection scheme for a climate model: description and moisture sensitivity. *Clim. Dyn.* **38**: 411–429. DOI: 10.1007/s00382-010-0972-2.

Klocke D, Pincus R, Quaas J. 2011. On constraining estimates of climate sensitivity with present-day observations through model weighting. *J. Climate* **24**: 6092–6099.

Knight CA, Miller LJ. 1998. Early radar echoes from small, warm cumulus: Bragg and hydrometeor scattering. *J. Atmos. Sci.* **55**: 2974–2992.

Kuang Z, Bretherton CS. 2006. A mass-flux scheme view of a high-resolution simulation of a transition from shallow to deep cumulus convection. *J. Atmos. Sci.* **63**: 1895–1909.

Kuo HL. 1962. On the controlling influences of eddy diffusion on thermal convection. *J. Atmos. Sci.* **19**: 236–243.

Lamontagne RG, Telford JW. 1983. Cloud-top mixing in small cumuli. *J. Atmos. Sci.* **40**: 2148–2156.

Lin C, Arakawa A. 1997. The macroscopic entrainment processes of simulated cumulus ensemble. Part 1: Entrainment sources. *J. Atmos. Sci.* **54**: 1027–1043.

Lovejoy S. 1982. Area-perimeter relation for rain and cloud areas. *Science* **216**: 4542, 185–187.

Ludlam FH, Scorer RS. 1953. Convection in the atmosphere. *Q. J. R. Meteorol. Soc.* **79**: 94–103.

Madden RA, Julian PR. 1971. Detection of a 40–50 day oscillation in the zonal wind in the tropical Pacific. *J. Atmos. Sci.* **5**: 702–708.

Mapes BE, Neale RB. 2011. Parameterizing convective organization. *J. Adv. Model Earth Syst.* **3**: M06004, DOI: 10.1029/2011MS000042.

Mironov DV. 2009. Turbulence in the lower troposphere: Second-order closure and mass-flux modelling frameworks. In *Interdisciplinary aspects of turbulence*. Springer-Verlag: Berlin. 161–221.

Morton BR, Taylor GI, Turner JS. 1956. Turbulent gravitational convection from maintained and instantaneous sources. *Proc. R. Soc. London A* **234**: 1–23.

Murphy JM, Sexton DH, Barnett DN, Jones GS, Webb MJ, Collins M, Stainforth DA. 2004. Quantification of modelling uncertainties in a large ensemble of climate change simulations. *Nature* **430**: 768–772.

Neggers RAJ, Siebesma AP, Jonker HJJ. 2002. A multiparcel method for shallow cumulus convection. *J. Atmos. Sci.* **59**: 1655–1668.

Neggers RAJ, Kohler M, Beljaars ACM. 2009. A dual mass flux framework for boundary layer convection. Part I: Transport. *J. Atmos. Sci.* **66**: 1464–1487.

Nordeng TE. 1994. 'Extended versions of the convective parameterization scheme at ECMWF and their impact on the mean and transient activity of the model in the Tropics'. Technical memorandum No. 206, ECMWF: Reading, UK.

Paluch IR. 1979. The entrainment mechanism in Colorado cumili. *J. Atmos. Sci.* **36**: 2467–2478.

Raga GB, Jensen JB, Baker MB. 1990. Characteristics of cumulus band clouds off the coast of Hawaii. *J. Atmos. Sci.* **47**: 338–355.

Randall DA, Huffman GJ. 1982. Entrainment and detrainment in a simple cumulus cloud model. *J. Atmos. Sci.* **39**: 2793–2806.

Randall DA, Krueger SK, Bretherton CS, Curry JA, Moncrieff M, Ryan BF, Miller MJ, Rossow WB, Tselioudis G, Wielicki B. 2003. Confronting models with data: The GEWEX Clouds Systems Study. *Bull. Amer. Meteorol. Soc.* **84**: 455–469.

Raymond DJ, Blyth AM. 1986. A stochastic mixing model for non-precipitating cumulus clouds. *J. Atmos. Sci.* **43**: 2708–2718.

Redelsperger J-L, Parsons DB, Guichard F. 2002. Recovery processes and factors limiting cloud-top height following the arrival of a dry intrusion observed during TOGA COARE. *J. Atmos. Sci.* **59**: 2438–2457.

Reuter GW. 1986. A historical review of cumulus entrainment studies. *Bull. Amer. Meteorol. Soc.* **67**: 151–154.

Rodts SMA, Duynkerke PG, Jonker HJJ. 2003. Size distributions and dynamical properties of shallow cumulus clouds from aircraft observations and satellite data. *J. Atmos. Sci.* **60**: 1895–1912.

Romps DM. 2010. A direct measurement of entrainment. *J. Atmos. Sci.* **67**: 1908–1927.

Romps DM, Kuang Z. 2010a. Do undiluted convective plumes exist in the upper tropical troposphere? *J. Atmos. Sci.* **67**: 468–484.

Romps DM, Kuang Z. 2010b. Nature versus nurture in shallow convection. *J. Atmos. Sci.* **67**: 1655–1666.

Seity Y, Brousseau P, Malardel S, Hello G, Bénard P, Bouttier F, Lac C, Masson V. 2011. The AROME-France convective-scale operational model. *Mon. Weather Rev.* **139**: 976–991.

Siebesma AP. 1998. Shallow cumulus convection. In *Buoyant Convection in Geophysical Flows*. Plate EJ, Fedorovich EE, Viegas XV, Wyngaard JC. (eds) Kluwer Academic Publishers: 441–486.

Siebesma AP, Cuijpers JWM. 1995. Evaluation of parametric assumptions for shallow cumulus convection. *J. Atmos. Sci.* **52**: 650–666.

Siebesma AP, Holtslag AAM. 1996. Model impacts of entrainment and detrainment rates in shallow cumulus convection. *J. Atmos. Sci.* **53**: 2354–2364.

Siebesma AP, Jonker HJJ. 2000. Anomalous scaling of cumulus cloud boundaries. *Phys. Rev. Lett.* **85**: 214–217.

Siebesma AP, Bretherton CS, Brown A, Chlond A, Cuxart J, Duynkerke PG, Jiang H, Khairoutdinov M, Lewellen D, Moeng C-H, Sanchez E, Stevens B, Stevens DE. 2003. A large-eddy simulation intercomparison study of shallow cumulus convection. *J. Atmos. Sci.* **60**: 1201–1219.

Siebesma AP, Soares P, Teixeira J. 2007. A combined eddy diffusivity mass-flux approach for the convective boundary layer. *J. Atmos. Sci.* **64**: 1230–1248.

Soares PMM, Miranda PMA, Siebesma AP, Teixeira J. 2004. An eddy-diffusivity/mass-flux parametrization for dry and shallow cumulus convection. *Q. J. R. Meteorol. Soc.* **130**: 3365–3384.

Squires P. 1958. The microstructure and colloidal stability of warm clouds. Part I. The relation between structure and stability. *Tellus* **10**: 256–261.

Squires P, Turner JS. 1962. An entraining jet model for cumulo-nimbus updraughts. *Tellus* **16**: 422–434.

Staniforth A, Wood N. 2008. Aspects of the dynamical core of a non-hydrostatic, deep-atmosphere, unified weather- and climate-prediction model. *J. Comput. Phys.* **227**: 3445–3464.

Stevens B, Ackerman AS, Albrecht BA, Brown AR, Chlond A, Cuxart J, Duynkerke PG, Lewellen DC, Macvean MK, Neggers RAJ, Sanchez E, Siebesma AP, Stevens DE. 2001. Simulations of trade-wind cumuli under a strong inversion. *J. Atmos. Sci.* **58**: 1870–1891.

Stommel H. 1947. Entrainment of air into a cumulus cloud. *J. Meteorol.* **4**: 91–94.

Stull RB. 1988. *An introduction to boundary-layer meteorology*. Kluwer Academic Publishers: London.

Sušelj KJ, Teixeira J, Chung D. 2011. A unified model for moist convective boundary layers based on a stochastic eddy-diffusivity/mass-flux approach. *J. Atmos. Sci.* submitted.

Taylor GR, Baker MB. 1991. Entrainment and detrainment in cumulus clouds. *J. Atmos. Sci.* **48**: 112–121.

Tiedtke M. 1989. A comprehensive mass flux scheme for cumulus parameterization in large-scale models. *Mon. Weather Rev.* **177**: 1779–1800.

Turner JS. 1963. The motion of buoyant elements in turbulent surroundings. *J. Fluid Mech.* **16**: 1–16.

Verzijlbergh RA, Heus T, Jonker HJJ, Vilà-Guerau de Arellano J. 2009. Turbulent dispersion in cloudy boundary layers. *Atmos. Chem. Phys.* **9**: 1289–1302.

Wagner TM, Graf HF. 2010. An ensemble cumulus convection parameterisation with explicit cloud treatment. *J. Atmos. Sci.* **67**: 3854–3869.

Wang Y, Geerts B, French J. 2009. Dynamics of the cumulus cloud margin: An observational study. *J. Atmos. Sci.* **66**: 3660–3677.

Warner J. 1955. The water content of cumuliform clouds. *Tellus* **7**: 449–457.

Weisman ML, Davis C, Wang W, Manning KW, Klemp JB. 2008. Experiences with 0–36 h explicit convective forecasts with the WRF-ARW model. *Weather Forecasting* **23**: 407–437.

Yanai M, Esbensen S, Chu J. 1973. Determination of bulk properties of tropical cloud clusters from large-scale heat and moisture budgets. *J. Atmos. Sci.* **30**: 611–627.

Yano J-I, Guichard F, Lafore J-P, Redelsperger J-L, Bechtold P. 2004. Estimations of mass fluxes for cumulus parameterizations from high-resolution spatial data. *J. Atmos. Sci.* **61**: 829–842.

Zhao M, Austin PH. 2005a. Life cycle of numerically simulated shallow cumulus clouds. Part I: Transport. *J. Atmos. Sci.* **62**: 1269–1290.

Zhao M, Austin PH. 2005b. Life cycle of numerically simulated shallow cumulus clouds. Part II: Mixing dynamics. *J. Atmos. Sci.* **62**: 1291–1310.

